

Molecular bridging of mitotic RanGTP and Aurora B kinase in the maintenance of kinetochore-microtubule attachments

Lee, Yoke Peng

2012

Lee, Y. P. (2012). Molecular bridging of mitotic RanGTP and aurora B kinase in the maintenance of kinetochore-microtubule attachments. Doctoral thesis, Nanyang Technological University, Singapore.

<https://hdl.handle.net/10356/50646>

<https://doi.org/10.32657/10356/50646>

**MOLECULAR BRIDGING OF MITOTIC RANGTP AND
AURORA B KINASE IN THE MAINTENANCE OF
KINETOCHORE-MICROTUBULE ATTACHMENTS**

LEE YOKE PENG

School of Biological Sciences

A thesis submitted to the Nanyang Technological University
in fulfillment of the requirement for the degree of
Doctor of Philosophy

2012

ACKNOWLEDGEMENT

I would like to express my sincere gratitude and appreciation to exceptional individuals whom without which, this project and thesis would not be possible.

Dr. Li Hoi Yeung, for being an understanding supervisor with constant support, guidance and advices.

Dr. Wong Chi Hang, for providing invaluable ideas and constructive discussion, as well as being a most supportive and encouraging post-doc.

My beloved family members, my ever-reliable girl friends; Catherine, Audrey, Ashley, Goh Lanpei, my good friends; Nor Hafiz Hassan and Edward Tan; SBS friends; Mary Chuah and Lew Yiliang, for their unwavering support, patience and understanding during the course of my Ph.D. study.

Dr. Lai Soak Kuan, for believing in and guiding me in my baby steps in research.

My lab colleagues; Kenny Chan, Anthony Ang, Yeap Szu Ling and Zhang Yucui, for their assistance and patience with me.

Lastly, I would like to thank the Academic Research Council, Ministry of Education, Singapore (Academic Research Fund AcRF Tier 1, RG37/08) and A*STAR, Biomedical Research Council (BMRC grant 08/1/22/19/568).

TABLE OF CONTENT

ACKNOWLEDGEMENT	I
TABLE OF CONTENT	II
ABSTRACT	IV
LIST OF ABBREVIATIONS	V
LIST OF FIGURES AND TABLES	VIII
Chapter 1 : Introduction	1
1.1 The cell cycle and mitosis	2
1.1.1 Cell cycle and cancer	7
1.2 Ran	7
1.2.1 Ran in spindle assembly	11
1.2.2 Spatial organization of nuclear proteins by Ran	11
1.2.3 Ran in chromosome congression	12
1.2.4 Ran at the spindle assembly checkpoint (SAC)	13
1.2.5 Ran at the kinetochores	13
1.2.6 Ran in nuclear envelope reformation	14
1.3 Kinetochore-microtubule attachments	17
1.3.1 Aurora B kinase	19
1.3.2 Mst1	20
1.4 tsBN2 cells in Ran studies	21
1.5 Fluorescence Resonance Energy Transfer (FRET) and the Rango biosensor	22
1.6 Aim of study	23
Chapter 2 : Materials and Methods	25
2.2 Time-lapse Imaging	27
2.3 FRET and Image Analysis	27
2.4 Immunofluorescence Microscopy	28
2.6 Spindle Microtubule Intensity (A.U.) and Relative Fluorescence Intensity Measurement	29
2.7 Western Blotting	30
2.9 Immunoprecipitation	31

Chapter 3 : Results	38
3.2 High RanGTP is important for the maintenance of proper chromosome alignment at the metaphase plate	42
3.3 RCC1 depletion causes misalignment of metaphase chromosome	47
3.4 RanGTP regulates the stability of kinetochore-microtubule attachments and prevents reactivation of the spindle assembly checkpoint prior to anaphase entry	54
3.5 Aurora B kinase activity is elevated in RanGTP-depleted cells.....	60
3.6 Aurora B kinase inhibitor ZM447439 quells the chromosome misalignment phenotype	64
3.7 Kinetochore proteins; Hec1 and RanGAP1, spindle proteins; TPX2 and dynactin p150, and chromokinesin Kid are unperturbed by changes in RanGTP at metaphase	69
3.8 RanGTP-dependent Crm1 directs Mst1 to the kinetochores	72
3.9 Functional Mst1 at the kinetochores maintains stable kinetochore-microtubule attachments.....	75
3.10 RanGTP-dependent Mst1 binds to and represses active Aurora B kinase activity.....	80
Chapter 4 : Discussion	85
4.1 <i>In vivo</i> FRET imaging revealed novel regulatory role of RanGTP at metaphase.....	86
4.2 Hyperactivated Aurora B kinase acts as an instigator to promote promiscuous kinetochore-microtubule attachments	88
4.3 Formation of RanGTP-Crm1-Mst1 ternary complex dictates the state of metaphase chromosome alignment	90
4.4 RanGTP-dependent regulation of Aurora B kinase determines its influence on kinetochore-microtubule attachments	92
4.5 RanGTP In Anti-cancer Therapies	95
REFERENCES	97

ABSTRACT

The multi-faceted RanGTPase has been implicated to be critically involved in nucleocytoplasmic transportation and cell cycle progression. However, the role of mitotic RanGTP in kinetochore-microtubule attachments at metaphase has yet to be described. Here, we report a molecular link between the mitotic RanGTP and Aurora B kinase in maintaining stable kinetochore-microtubule attachments after proper chromosome congression. *In vivo* FRET imaging revealed that real-time decay in RanGTP levels at metaphase is coupled with a progressive displacement of pre-aligned chromosomes from the cell equator. An enrichment of mitotic RanGTP is necessary for recruitment of Mst1 to restrict Aurora B kinase's influence in promoting reorientation of kinetochore-microtubule attachments at the kinetochores. By ensuring the precision of metaphase chromosome alignment prior to chromosome segregation, this additional role of the RanGTP underscores its significance in protecting genomic integrity and preserving the fidelity of mitotic progression.

LIST OF ABBREVIATIONS

bp	base pair
°C	degree Celcius
<i>g</i>	g-force or relative centrifugal force
hr	hour
kDa	kilodalton
mg	milligram
min	minute
μm	micrometer
mm	millimeter
mM	millimolar
nM	nanomolar
rpm	revolutions per minute
%	Percent
μg	microgram
μl	microlitre
ACA	Anti-centomere antigens
APC	Anaphase promoting complex
A.U.	Arbitrary unit
BSA	Bovine serum albumin
Cdc	Cell division cycle
Cdk	Cyclin dependent kinase
CFP	Cyan fluorescent protein
Crm1	Chromosome region maintenance 1

DAPI	4',6-diamidino-2-phenylindole, nuclei marker
DMSO	Dimethyl sulfoxide
DMEM	Dulbecco's Modified Eagle's Medium
DNA	Deoxyribonucleic acid
DTT	Dithiothreitol
EDTA	Ethylenediamine tetraacetic acid
EGTA	Ethylene glycol tetraacetic acid
FRET	Fluorescence resonance energy transfer
GFP	Green fluorescent protein
HEPES	4-(2-hydroxyethyl)-1-piperazineethanesulfonic acid
HRP	Horse radish peroxidase
H2B	Histone-2B
IgG	Immunoglobulin G
K	Lysine
Mst1	Mammalian sterile 20-like protein kinase 1
NaCl	Sodium chloride
NES	Nuclear export signal
PAGE	Polyacrylamide gel electrophoresis
PBS	Phosphate-buffered saline
R	Arginine
RanBP1	Ran-binding protein 1
RanGAP1	Ran-GTPase activating protein 1
RCC1	Regulator of chromosome condensation 1
RT	Room temperature
SAC	Spindle assembly checkpoint

SDS	Sodium dodecyl sulphate
TBST	Tris-buffered saline with tween-20
WT	Wild-type
YFP	Yellow fluorescent protein

LIST OF FIGURES AND TABLES

Figure 1.1: The cell cycle, cell cycle checkpoints and the distinct phases of mitosis.....	6
Figure 1.2: Regulation of RanGTP and its distinct distribution during interphase and mitosis.....	10
Figure 1.2.1: Schematic depiction of established functions of RanGTP in mitosis.	16
Figure 1.3: Types of kinetochore-microtubule attachments.....	18
Figure 1.5: The FRET biosensor, Rango and its detection of RanGTP. .	22
Figure 3.1: FRET biosensor, Rango, as a RanGTP indicator.....	41
Figure 3.2.1: Schematic depiction of the experimental conditions.....	42
Figure 3.2.2: Incubation of tsBN2 cells at non-permissive temperature causes decline in RanGTP levels and compromises the maintenance of metaphase chromosome alignment.	44
Figure 3.3.1: RCC1 depletion at non-permissive temperature causes misalignment of metaphase chromosome without affecting spindle structure.	48
Figure 3.3.2: RCC1 is efficiently depleted at non-permissive temperature.	49
Figure 3.3.3: Complementation with wild-type RCC1 reinstated proper metaphase chromosome alignment at non-permissive temperature.	51
Figure 3.3.4: Functionally active RanGTP is crucial for stable chromosome alignment at metaphase.	53
Figure 3.4.1: Aberrantly aligned chromosomes are composed of metaphase chromosomes with intact sister chromatids.....	55
Figure 3.4.2: Mitotic RanGTP is required for stable attachment of microtubules to the kinetochores.....	57
Figure 3.4.3: Mitotic RanGTP is necessary to prevent untimely reactivation of the spindle assembly checkpoint.....	59
Figure 3.5.1: Active Aurora B kinase phosphorylation at Thr232 after RanGTP depletion.....	61
Figure 3.5.2: Diminished mitotic RanGTP enhances Aurora B kinase activity.	62
Figure 3.6.1: Phosphorylation of Aurora B kinase is sufficiently inhibited by Aurora B kinase inhibitor, ZM447439.	64
Figure 3.6.2: Aberrant Aurora B kinase activation compromises the fidelity of metaphase chromosome alignment.	66
Figure 3.6.3: Regulated Aurora B kinase activation curbs the chromosome misalignment phenotype.....	68
Figure 3.7.1: Localization of spindle protein TPX2, kinetochore proteins Hec1 and RanGAP1, and spindle motor dyxactin-p150 are unaltered by RanGTP disruption.....	70
Figure 3.7.2: Chromokinesin Kid is not depleted after RanGTP depletion.	71
Figure 3.8.1: Mitotic effector Crm1 is significantly reduced from the kinetochores after RanGTP disruption.....	72
Figure 3.8.2: RanGTP-dependent Crm1 shuttles Mst1 to the kinetochores.	74

Figure 3.9.1: Overabundant of wild-type Mst1 restores the stability of kinechore-microtubule attachment for proper metaphase chromosome alignment.	76
Figure 3.9.2: Mst1 is indispensable to maintain proper chromosome alignment at metaphase.	78
Figure 3.9.3: Mst1 depletion compromises stable metaphase chromosome alignment in HeLa cells.	79
Figure 3.10.1: Robust interaction of functionally active Mst1 with Aurora B kinase.	81
Figure 3.10.2: Wild-type Mst1 represses active Aurora B kinase activity.	82
Figure 3.10.3: Functionally intact Mst1 is recruited to kinetochores of metaphase chromosomes.	84
Figure 4.4: Model illustrating the role of mitotic RanGTP in preserving stable chromosomal alignment during metaphase.	94
 Table 1. Antibodies Used	 33
Table 2. Plasmids Used	37

Chapter 1 : Introduction

1.1 The cell cycle and mitosis

The most recurring process that actively proliferating cells undergo is the cell cycle, in which, a cell grows, duplicates its DNA and divides into two genetically identical daughter cells. These processes depict the two major phases of the cell cycle: the S phase, where in genetic materials double, and the M phase where in nuclear materials and cellular components are equally segregated and distributed into two identical daughter cells. Flanking these two phases are gap or growth phases known as the G1 and G2 phases. The G1, S and G2 phases collectively form interphase, while the M phase constitutes mitosis and cytokinesis (Fig. 1.1).

In most metazoans, mitosis is a relatively transient but potentially most vital event in a cell's lifetime. Growth and synthesis processes during interphase occur in preparation for mitosis. Mitosis is made up of five phases: prophase, prometaphase, metaphase, anaphase and telophase. As a cell enters prophase, chromatin fibers begin to condense and astral microtubules emanate from the centrosomes, thus pushing the duplicated centrosomes to opposite sides of the cell [1]. At prometaphase, the nuclear envelope (NE) disassembles and spindle microtubules from the centrosome begin to search and attach to the kinetochores of chromosomes. At metaphase, chromosomes are at their most tightly condensed form and the sister chromatids are held by spindle microtubules from opposite poles of the mitotic spindle. As a consequence of the counterbalance of the opposing tension exerted by spindle microtubules on kinetochores of sister chromatids, chromosomes are evenly aligned along the equatorial plane of the spindle, which is the metaphase plate. Next, at anaphase, sister chromatids separate

and are pulled apart by shortening kinetochore microtubules. Thereafter, the spindle poles move apart, further promoting sister chromatids separation. Mitosis concludes with telophase. During telophase, daughter chromosomes arrive at opposite spindle poles and decondense. In addition, nuclear envelope reassembles around each set of daughter chromosomes. Finally, at cytokinesis, a cleavage furrow forms between the two nucleus and pinches the parent cell into two daughter cells, each with its individual nucleus (Fig. 1.1).

Judging from the intricateness of the mitotic process, it is logical that regulatory mechanisms are present to protect the fidelity of mitosis and the cell cycle as a whole. Two primary cell cycle control systems are set in place to monitor and regulate the progression of the cell cycle: a family of kinases known as the cyclin-dependent kinases (Cdks) and a set of checkpoints which are collectively referred to as the cell cycle checkpoints.

As the name suggests, Cdks are dependent on and function in cooperation with a set of proteins known as cyclins. Whilst Cdks are expressed constitutively, cyclin protein levels fluctuate over the course of the cell cycle in response to various molecular cues. Entry into mitosis, for example, is driven by the decline in S-Cdk (complex of Cdk1 and its partner cyclin A) activity and the elevation in M-Cdk (complex of Cdk1 and cyclin B) activity, which triggers a cascade of phosphorylation leading to NE breakdown, chromosome condensation etc, characteristic of mitotic onset [2]. As mitosis progresses, M-Cdk activity declines as the M-cyclin is degraded and its role is taken over by another Cdk-cyclin pair. Therefore, Cdks, with

their specific cyclin partners, can ensure that the cell cycle occurs sequentially and in a unidirectional manner.

Meanwhile, the cell cycle checkpoints hold a more supervisory role, preventing entry into the next stage of the cell cycle unless specific checkpoint requirements are satisfied. Taking the spindle assembly checkpoint (SAC), for example. The SAC functions at the metaphase to anaphase transition. It is an active signal produced by unattached or improperly attached kinetochores to halt mitotic progression into anaphase. In the absence of proper kinetochore attachments and balanced tension across the kinetochore, a 'wait-anaphase' signal is generated [3,4,5]. SAC components, namely Mad2, BubR1 and Bub3, sequester Cdc20, forming the mitotic checkpoint complex (MCC) that persists at the kinetochore and renders the anaphase promoting complex (APC) inactive [6]. Only when all kinetochores have achieved amphitelic attachments, positive effector Cdc20 binds to and activates the APC, triggering a cascade of events that culminates with sister chromatid segregation and thus mark anaphase onset.

Whilst the SAC functions at mitosis, distinct checkpoints are set in place in each of the three phases of interphase: the G1, S and G2 checkpoints. Collectively, and rather aptly, these checkpoints are also known as DNA damage checkpoints as they crucially monitor the fidelity of genetic materials earmarked for duplication and subsequent inheritance by daughter cells. Arrest at the G1 checkpoint allows for repair of any mutated or damaged bases prior to DNA replication at S phase whilst the G2 checkpoint repairs double-stranded DNA breakages, if any, before entry into mitosis [2]. When DNA damage is detected in a cell, a DNA damage response is

triggered via the ATM/ATR and p53 pathway to trigger checkpoint arrest and allow time for damage repair. Not surprisingly, this occurs by inhibition of specific downstream interphase cdk-cyclin pairs regulating cell cycle progression [7,8].

However, in the event of severe irreparable DNA damage at the DNA damage checkpoints or persisted spindle defect at the SAC, another regulatory mechanism takes over and apoptosis occurs instead to prevent propagation of aneuploid cells. Despite the aforementioned mechanisms present to preserve the fidelity of cell cycle progression and to safeguard the genome, some genetically defective cells can evade the scrutiny of the checkpoints and escape cell death. As such, these cells may acquire genetic defects, which predisposes cancerous transformation.

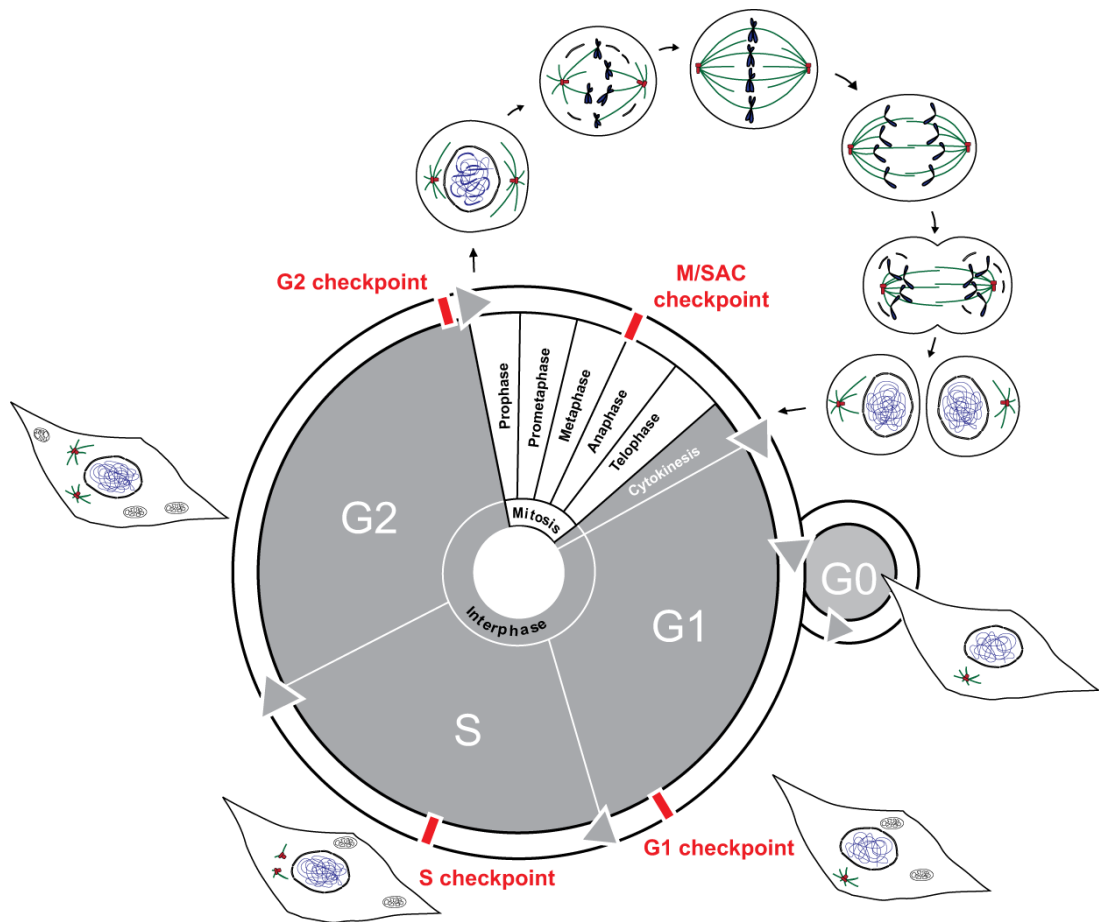


Figure 1.1: The cell cycle, cell cycle checkpoints and the distinct phases of mitosis.

The cell cycle consists of interphase and M phase. Interphase is made up of two growth phases (G1 and G2 phases) and a DNA replication phase (S phase). At M phase, genetic materials (mitosis) and cellular components (cytokinesis) are equally segregated to daughter cells. The 5 phases of mitosis are namely prophase, prometaphase, metaphase, anaphase and telophase. Cytokinesis occurs at the end of mitosis and marks the end of a cell cycle. These cell cycle phases are kept in check by cell cycle checkpoints to preserve the fidelity of cellular processes and mitotic progression.

1.1.1 Cell cycle and cancer

Cancer is a disease of inappropriately dividing tumor cells.

Tumorigenesis in itself is a multi-step evolutionary process in which a normal cell acquires selective advantage to divide uncontrollably and potentially develop into a cancerous mass. Although regulatory mechanisms are present to ensure that the cell cycle occurs at almost perfect accuracy and precision, tumor cells have the ability to manipulate and bypass these stringent controls to achieve replicative immortality. For example, slippage of SAC arrest and premature anaphase entry commonly found in lung and colon tumors are due to haploinsufficiency or downregulation of SAC components BubR1, Mad2 and Bub1 [9,10,11]. As a consequence, aneuploid daughter cells with genetic instability are generated and predisposed to tumor progression. In addition, tumor cells have shown defects in cell cycle processes governed by a GTPase Ran, which will be discussed in detail below.

1.2 Ran

The small GTPase Ran has multifaceted roles in cell cycle progression. Functionalities of Ran hinges on its nucleotide state, whereby the GTP-bound form and GDP-bound form are established by the activities of guanine exchange factor RCC1 (Regulator of Chromosome Condensation 1) and cytoplasmic RanGAP1 together with RanBP1.

Chromatin-bound RCC1 is the sole exchange factor for generation of RanGTP. Although RCC1 can catalyze the exchange of Ran from GDP to GTP and vice versa, it has no preference for either forms of Ran. However, due to the significantly higher concentration of intracellular GTP compared to

GDP, RCC1 preferentially loads GTP to Ran. In addition, the localization of RCC1 to chromatin is enhanced by its interaction with RanGTP, thus promoting the directionality of exchange towards RanGTP formation (Fig. 1.2A) [12].

In the nucleus, RanGTP can bind to both import and export factors. Association of RanGTP with import factor importin- β mediates release of import cargoes brought in by importin- β . Meanwhile, interaction of RanGTP with export factor, Crm1, facilitates transport of nuclear proteins to the cytoplasm. Upon entry into the cytoplasm, hydrolysis of Ran from its active to inactive conformation occurs via its interaction with RanGAP1 and RanBP1. Although both RanGAP1 and RanBP1 are predominantly cytoplasmic, they show enrichment at the cytoplasmic side of the NE, which may serve as a preferred site of hydrolysis on RanGTP [13].

The distinct localization of these Ran regulators across the NE, coupled with the active nuclear import of Ran, creates a high concentration of RanGTP in the nucleus and a low concentration in the cytoplasm [14]. The distribution of RanGTP in a cell is often referred to as a gradient and this is especially distinct in mitotic cells following NE breakdown, with a high RanGTP level surrounding RCC1-associated chromosomes and progressively decreasing towards the cell periphery (Fig. 1.2B) [15]. This gradient dictates many of the established Ran functions: during interphase, Ran regulates the directionality of nucleocytoplasmic transport; and in mitosis, Ran is involved in mitotic spindle assembly, nuclear organization, chromosome congression, nuclear envelope reformation and regulation of cell cycle transitions.

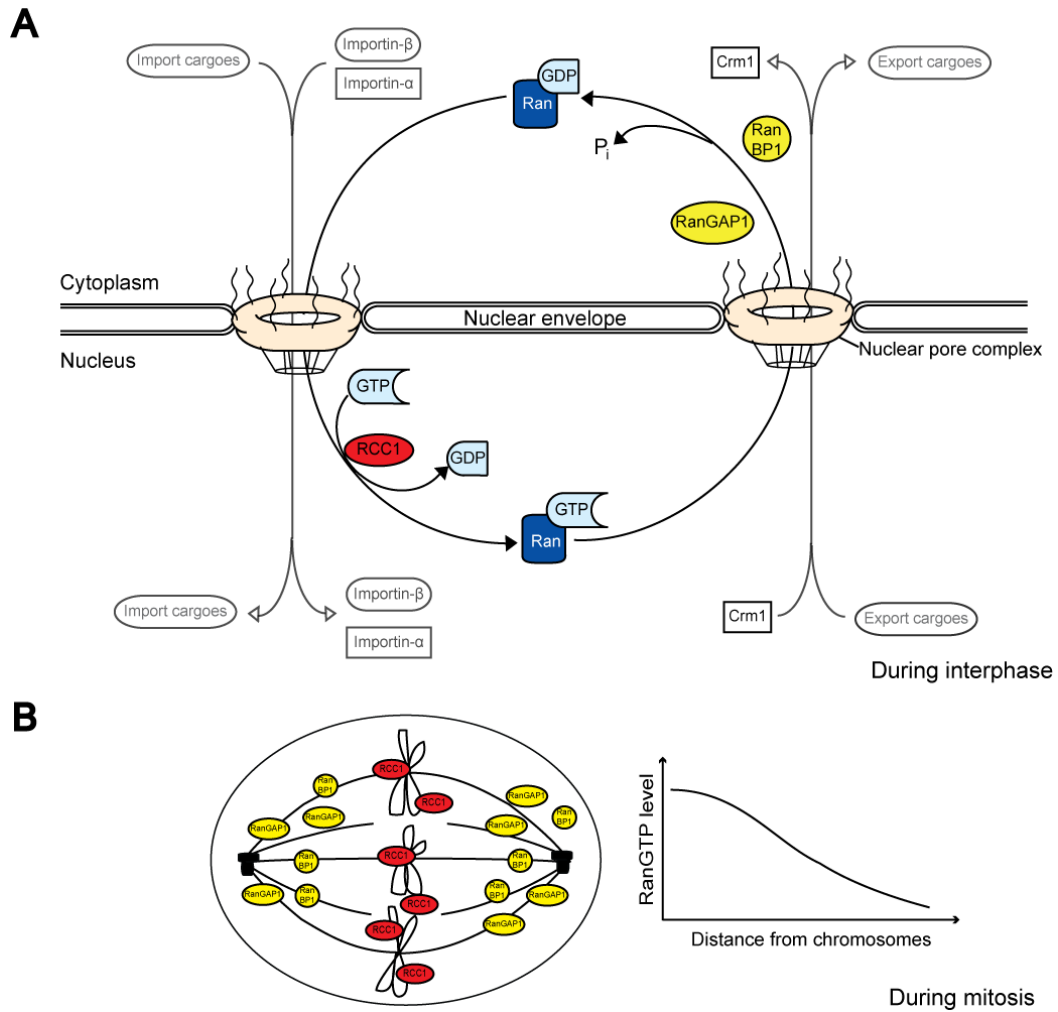


Figure 1.2: Regulation of RanGTP and its distinct distribution during interphase and mitosis.

A) During interphase, RanGTP is formed in the nucleus by chromatin-bound RCC1 and is hydrolyzed to RanGDP in the cytoplasm by RanGAP1 and RanBP1. B) During mitosis, RCC1 is bound to the condensed chromosomes while RanGAP1 and RanBP1 are distributed more distant from the chromosomes. Graph shows RanGTP level in a mitotic cell, from the metaphase plate to the periphery.

1.2.1 Ran in spindle assembly

Early research on Ran's importance was performed on *Xenopus* egg extracts. High levels of RanGTP were shown to stimulate formation of microtubule asters and spindle-like structures in the extracts even in the absence of DNA [16]. RanGTP was also found to regulate microtubule dynamics in mitosis: promoting microtubule nucleation, stabilization and control of microtubule-associated motor proteins, favouring spindle formation [17,18]. Findings from *Xenopus* egg extracts, coupled with computer simulations, indicate that high levels of RanGTP surrounding condensed chromosomes favours microtubule nucleation whereas lower levels of RanGTP more distant from chromosomes favours microtubule stabilization [19]. Subsequently, the role of Ran *in vivo* was established in somatic cells with the use of Ran and RCC1 mutants, whereby disruption on the Ran gradient leads to defective spindles and aberrant chromosome alignment [20,21].

1.2.2 Spatial organization of nuclear proteins by Ran

Meanwhile, proper spindle formation is also dependent on protein factors recruited and activated by RanGTP. Elevated levels of RanGTP within the proximity of chromosomes provide a spatial cue for activation of these factors by liberating them from inhibition by importin- α and/or importin- β . Spindle assembly factors (SAFs) and Ran regulators, RanGAP1 and RanBP1, are then recruited to structures like spindle poles and kinetochores to facilitate spindle formation and mitotic progression [14,22].

All SAFs control microtubule dynamics in distinct ways but are interdependent for activation. For example, TPX2, which functions in microtubule nucleation, targets motor protein XKLP2 to microtubule minus ends, activates Aurora A kinase and forms complex with other SAFs such as Eg5 and HURP. Aurora A kinase, in turn, phosphorylates other SAFs, forming a 'phosphorylation gradient' for progressive activation of the plethora of SAFs for spindle formation [15]. Failure to recruit these protein factors has been shown to result in multipolar spindles, defocused spindles and aberrant midzone formation [23].

1.2.3 Ran in chromosome congression

RanGTP also regulates chromosome congression, in relation to its role in spindle formation and organization of nuclear proteins. In a novel association of lamin B with mitotic spindles, disruption of RanGTP levels has been shown to result in defective spindles or spindles lacking chromosome congression [24]. In a separate experiment, in extracts depleted of SAF component, XKid, bipolar spindles are able to form but chromosomes fail to congress [23,25]. Meanwhile, the expression Ran mutants, RanT24N (dominant negative) or RanQ69L (dominant positive) in mitotic cells showed increase in frequency of cells with bipolar spindles but with aberrant chromosome alignment [26]. These experiments, although indirect, suggest an involvement of Ran in ensuring proper chromosome congression.

1.2.4 Ran at the spindle assembly checkpoint (SAC)

At the SAC, localization of spindle checkpoint components at the kinetochores is sensitive to RCC1 and RanGTP concentration. When multifold of exogenous RCC1 is added to metaphase cells, significant loss of checkpoint proteins was detected, resulting in a silenced checkpoint. However, an active SAC was reinstated when recombinant RanGAP1 was added to counterbalance the RCC1 activity and restore a moderate RanGTP concentration [27]. In a separate experiment, fluorescence recovery after photobleaching (FRAP) showed that RCC1's binding to chromatin is highly dynamic during metaphase and this association stabilizes towards anaphase [28]. As such, the SAC can be maintained at metaphase without slippage, consistent with the aforementioned study that elevated levels of RCC1 and RanGTP can override the spindle checkpoint and restore the proteolytic activity of the APC for progression to anaphase. These findings thus implicate RanGTP's role at the SAC.

1.2.5 Ran at the kinetochores

On a different spectrum, whilst the RanGTP gradient crucially directs nucleocytoplasmic transport during interphase, the absence of nuclear envelope during mitosis renders this process obsolete. Nonetheless, proteins associated to the transport machineries have been shown to be actively involved in the progression of mitosis. For example, the nuclear export receptor Crm1 switches its role from an export factor to a regulator of mitosis. It recognizes nuclear export signal (NES)-bearing mitotic regulators such as survivin and Nup358 and thus forming a ternary complex with RanGTP to

allow for shuttling and distinct localization of the NES-bearing proteins [29,30,31]. Interestingly, Crm1 together with Ran regulator RanGAP1 are localized to the kinetochores during mitosis. Complexes of RanGTP, Crm1, and RanGAP1 or NES-bearing proteins have been shown to be involved in microtubule nucleation at the kinetochores for mitotic spindle assembly [32,33].

1.2.6 Ran in nuclear envelope reformation

As mitosis ends, mitotic spindle disassembles and NE forms around the decondensing chromosomes. RanGTP dictates this reassembly of the NE. Proof of Ran's role in NE assembly was established when artificial beads coated with Ran GTPase added to *Xenopus* egg extracts were shown to induce the formation of NE-like structures on the surface of the beads in the absence of chromatin [34]. Moreover, the importance of the Ran cycle is highlighted in NE assembly whereby non-convertible Ran mutants, RanQ69L and RanT24N, both fail to induce NE formation while addition of RCC1 or RanGTP allows for formation of double membrane NE [35].

Judging from the aforementioned roles of Ran, it is undeniable whilst small, this protein has far-reaching and prominent influences in orchestrating major aspects of the cell cycle. In regulating multiple key steps in mitosis, from the initial mitotic spindle formation to nuclear envelope reformation as mitosis concludes (Fig.1.2.1), these functions of Ran renders it indispensable to the preservation of the fidelity of mitotic progression and the stability of the genome from one generation to the next. Therefore it is not surprising that

cancer cells in particular, exhibit multiple dysregulations in RanGTP pathways involving mutations and perturbations to expressions of multiple proto-oncogenes [36,37].

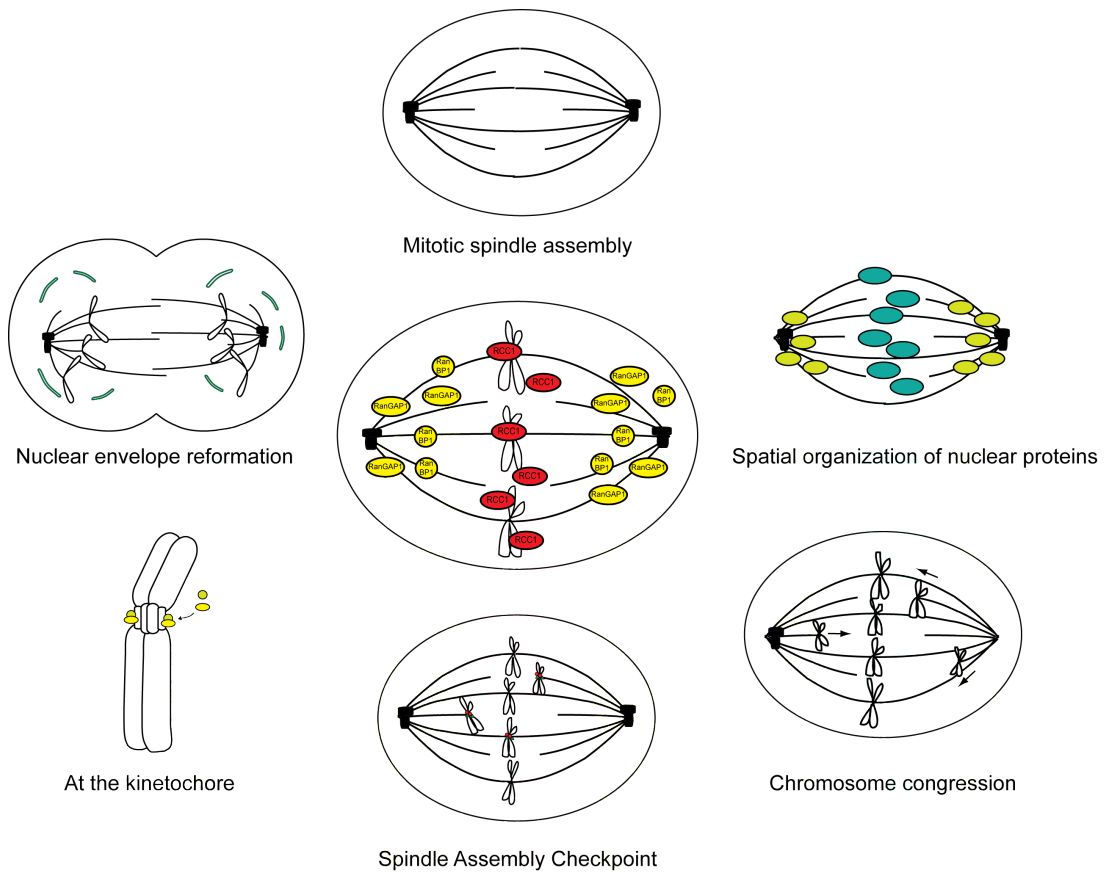


Figure 1.2.1: Schematic depiction of established functions of RanGTP in mitosis.

Clockwise from top : In the assembly of the mitotic spindle, in the organization of nuclear proteins based on the mitotic RanGTP gradient, during chromosome congression, at the spindle assembly checkpoint (SAC), involvement at the kinetochores and during the nuclear envelope reformation.

1.3 Kinetochore-microtubule attachments

Central to this theme is the KMN network (KNL1-Mis12-Ndc80/Hec1). The KMN network forms the core of the microtubule-binding site at the kinetochores and acts as a platform for the establishment of the initial kinetochore-microtubule contact [38]. Functionally indispensable, components of the network are highly conserved. Depletion of any of the KMN components results in erroneous attachments and defective chromosome alignment [39,40]. The Ndc80 complex in particular, is extensively being studied and has been suggested to be responsible for the conversion of initial lateral kinetochore-microtubule attachments to end-on attachments [41]. In addition, recent cryo-EM reconstructions of the Ndc80 complex has further shed light into the precise contact points of the initial kinetochore-microtubule attachments and lend credence to the aforementioned postulation [42,43].

Apart from establishing kinetochore-microtubule contact, it is also crucial to ensure that the attachments formed are correct. For proper alignment at the metaphase plate, stable end-on amphitelic attachments must be achieved (Fig.1.3). In amphitelic attachments, both tension balance and kinetochore occupancy requirements are fulfilled and this allow for mitotic progression through the SAC. However, improper attachments do occur. Briefly, monotelic attachment occurs when a chromosome is attached at only one kinetochore, syntelic attachment occurs when both kinetochores are attached to microtubules from the same pole, and merotelic attachment occurs when a kinetochore is attached to microtubules from both poles [44,45]. Such attachments, if left unchecked, can results in missegregation errors and result in aneuploid cells. Therefore, it is vital that these improper

attachments are picked up and are corrected. Amongst the key players for this role are the chromosome passenger proteins (CPCs), which consist of Aurora B kinase, INCENP, survivin and borealin. Of interest, the role of Aurora B kinase at the kinetochore will be described in further detail below.

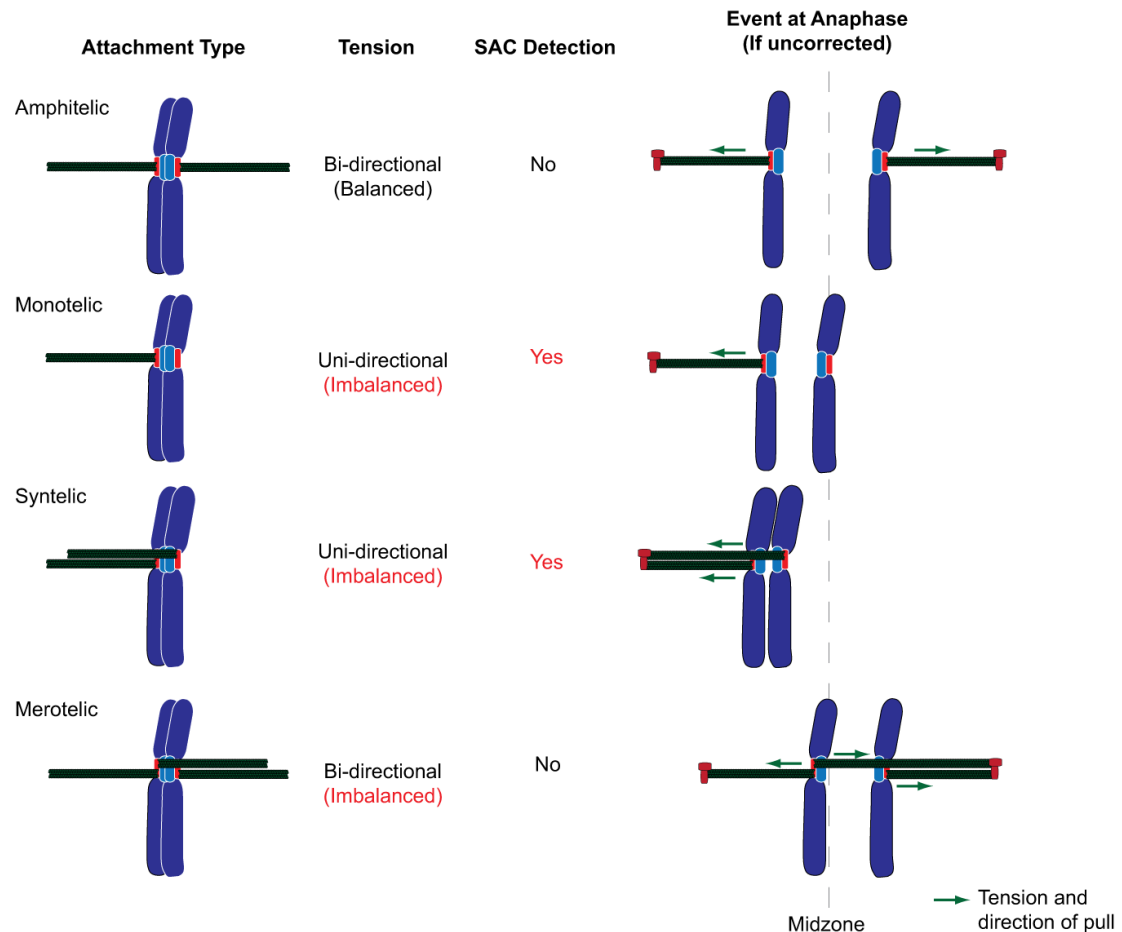


Figure 1.3: Types of kinetochore-microtubule attachments.

Some of the more common types of kinetochore-microtubule attachments. Amphitelic attachment represents the proper attachment with balanced tension across the kinetochores for stable alignment of chromosomes at the equator and equal segregation of sister chromosomes. Monotelic, syntelic and merotelic attachments do not satisfy the tension requirement and thus is susceptible to detection by the spindle assembly checkpoint. If left uncorrected, such erroneous attachment types can results in aneuploid daughter cells.

1.3.1 Aurora B kinase

Aurora B kinase, a major regulator of mitosis, is sensitive to tension across the kinetochores and thus henceforth key to detect and rectify erroneous kinetochore-microtubule attachments when chromosomes are congressing. Therefore, it is not surprising that it is found to be more abundant at prometaphase when proper kinetochore-microtubule attachments have not been established [46,47]. Notably, active Aurora B kinase has been found to be enriched on kinetochores with merotelic attachments [48].

In addition, as a member of the CPC, Aurora B kinase is responsible for the recruitment and regulation of kinetochore proteins, including components of the SAC (Bub1, BubR1, and CENP-E) and those involved in kinetochore-microtubule interactions (MCAK, Ska, and Hec1) [47,49,50]. Via autophosphorylation and phosphorylation of proximal kinetochore substrates such as Hec1 and KNL-1, this kinase modulates the lability of improperly attached kinetochore-microtubule fibers and ensures sister chromosomes are properly attached to spindle microtubules at the kinetochores [51,52,53]. In a recent report, the mechanism by which Aurora B kinase executes its error correction role was further deciphered through the modulation of the interaction between the Ska complex and KMN network. By antagonizing Ska protein localization on improperly attached kinetochores, kinetochore-microtubule reorganization occurs to allow for proper end-on attachment to eventually form [54]. Similarly, the localization and activity of MCAK is also negatively regulated by Aurora B kinase to modulate MCAK's microtubule depolymerization activity, likely to stabilize amphitelic attachments formed [46].

In line, Aurora B kinase also has a role at the SAC, at which it cooperates with SAC protein Bub1 to maintain the SAC, likely persisting the mitotic arrest until all proper kinetochore-attachments are achieved [55].

1.3.2 Mst1

Mst1 (mammalian Ste20-like kinase 1) is an established Ran-dependent NES-bearing cargo, which has been implicated in cell proliferation, cell survival and lineage specification [56,57,58]. Mst1 activation at apoptosis, its most characterized function, involves cleavage of the C-terminal domain. Upon cleavage, the N-terminal is liberation from inhibition by the C-terminal domain that also bears two putative NES. This allows translocation of the active N-terminal kinase domain into the nucleus to induce chromatin condensation and DNA fragmentation, which are characteristic of apoptosis [59]. Whilst Mst1's role in apoptosis is more established, the precise mechanism by which this kinase exerts its influence on other processes remains largely unknown with only a handful of known substrates that have been characterized.

Recently, Mst1 was shown to have a novel regulatory function in mitosis, in modulating kinetochore-microtubule attachments. By regulating the activity of Aurora B kinase, Mst1 is therefore involved in ensuring accurate kinetochore-microtubule attachments for precise segregation of chromosomes and maintenance of genomic integrity [52].

1.4 tsBN2 cells in Ran studies

Although most early Ran studies conducted in *Xenopus* extracts and yeast provided vital information on Ran's importance, there was a need for the establishment of Ran's roles *in vivo*, in somatic cells. As such, studies on Ran shifted slightly to the use of RCC1 or Ran mutants and silencing RNAs (siRNAs) in mammalian cells such as HeLa and tsBN2 cells [20,60,61].

Chinese hamster cell line tsBN2 that has a temperature sensitive mutation in the RCC1 allele is commonly used in the study of RCC1 and Ran in somatic cells. This cell line was developed by Nishitomo et. al. from the BHK21 cell line to study the occurrence of premature chromosomes condensation [62,63]. The RCC1 allele in tsBN2 cells bears a point mutation, which results in a single amino acid change in the RCC1. Upon temperature shift to non-permissive temperature, the structure of RCC1 is altered and endogenous RCC1 is largely depleted [62,64]. In the absence of RCC1, RanGTP is no longer regenerated and the more predominant RanGDP form accumulates, thereby acting as a RanGTP-deficient system to allow for *in vivo* study of RanGTP perturbations in mammalian cells [65].

1.5 Fluorescence Resonance Energy Transfer (FRET) and the Rango biosensor

Visualization of RanGTP/GDP distribution is crucial in the understanding of Ran's role and importance. FRET is commonly used to map RanGTP. FRET is a technique that allows energy transfer between two different fluorophores at close proximity (0.002-0.01 μ m). Excitation of donor fluorophore, allows transfer of donor emission energy to excite a nearby acceptor fluorophore resulting in FRET. Novel FRET biosensor, Ran-regulated importin- β cargo (Rango), allows analysis of RanGTP levels based on intramolecular interaction between importin- β with either Rango or RanGTP. Rango is made up of a snurportin-derived importin- β binding (IBB) domain flanked by the yellow fluorescent protein (EYFP) and cerulean cyan fluorescent protein (CFP) at its ends. The IBB domain, when bound to importin- β , sterically prevents the ends from interacting. In the absence of importin- β , when importin- β is bound to RanGTP, the EYFP and CFP ends come into close contact and can undergo intramolecular FRET, indicating the presence of RanGTP (Fig. 1.5)[61].

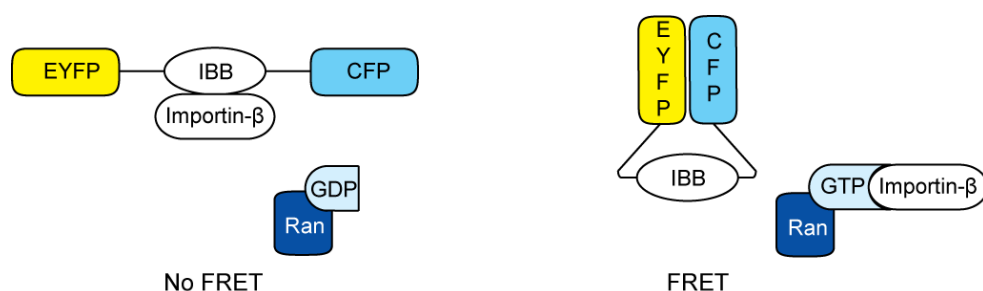


Figure 1.5: The FRET biosensor, Rango and its detection of RanGTP. Conformations of the Rango biosensor in the presence and absence of RanGTP are shown. In the absence of RanGTP, importin- β is bound to the IBB domain and the Rango biosensor is in an extended conformation. Thus no FRET occurs. In the presence of RanGTP, importin- β is liberated from the IBB domain and therefore allows the EYP and CFP to come into close contact and undergo intramolecular FRET.

1.6 Aim of study

Mitosis presents as a good target for anti-cancer therapy. Errors in mitosis, if left unchecked will give rise to aneuploid daughter cells with genetic instability, which has the potential to grow into a cancerous mass. At present, many anti-mitotic drugs have been developed and some have been applied with sufficiently high efficacy [66]. Given that the mitotic GTPase Ran is implicated in regulating multiple key processes in mitosis, it is logical to consider this protein as a potential biomarker and/or target for development of anti-cancer therapeutics.

In this study of RanGTP in mitosis, temperature sensitive tsBN2 cells were used and by treating them with MG132, cells were arrested at metaphase without affecting mitotic spindle formation or chromosome congression. Upon increase in temperature to non-permissive temperature of 39.5°C, live cell FRET time-lapse imaging showed that the real-time decline of RanGTP levels at metaphase is coupled with a progressive displacement of pre-aligned metaphase chromosomes from the cell equator. As the cells were pre-arrested at metaphase with proper chromosome alignment prior to the depletion of RanGTP, the observed chromosome misalignment phenotype was unexpected. Therefore, this prompted us to look into whether RanGTP may be involved in the maintenance metaphase chromosome alignment.

With the application of *in vivo* FRET imaging and evidences from biochemical studies, we report a molecular link between the mitotic RanGTP and Aurora B kinase in the maintenance of stable kinetochore-microtubule attachments after chromosome congression at metaphase. A high local

accumulation of mitotic RanGTP is necessary to restrict Aurora B kinase's influence on the lability of kinetochore-microtubule dynamics, through recruitment of and the antagonistic activity of Mst1 at the kinetochores. This role of RanGTP fills the chronological gap between chromosome congression and segregation, further strengthening its role as a master regulator of mitosis and protector of genomic integrity.

Considering that several downstream effectors of RanGTP, including Aurora kinases, are already being targeted and the anti-cancer agents are being tested at the clinical stage, this study provides further support for RanGTP as a wide-ranging mitotic biomarker and target to eradicate highly proliferative cells with skewed RanGTP level in anti-cancer therapeutics.

Chapter 2 : Materials and Methods

2.1 Cell Culture and Drug Treatments

tsBN2 cells were grown in DMEM (Gibco, Invitrogen, USA) containing 10% fetal bovine serum (Hyclone) and 1% Penicillin/Streptomycin (Gibco) in a humidified atmosphere with 5% carbon dioxide, at 33.5°C (permissive temperature). The non-permissive temperature used was 39.5°C. HeLa cells and HEK cells were cultured in similar conditions but at 37°C. For MG132 treatment, 20mM MG132 (Sigma, USA) in dimethyl sulfoxide (DMSO) stock was diluted in medium to a working concentration of 10 μ M. Cells were treated with 10 μ M of MG132 prior to incubation at permissive (33.5°C) or non-permissive temperature (39.5°C) in experiments. Aurora B kinase inhibitor, ZM447439 (Tocris Biosciences, USA), was dissolved in DMSO to a stock concentration of 100mM, and dissolved in DMEM to a working concentration of 500nM. Transient transfection of Rango, histone H2B (H2B)-mCherry, H2B-GFP, tubulin-mCherry, wild-type (WT) RCC1-GFP, Mst1 WT-mCherry, Mst1 K59R-mCherry, Mst1 K59R Δ C-mCherry, Aurora B kinase-GFP, FLAG, FLAG-Mst1 WT and/or Flag-Mst1 K59R Δ C plasmids were performed using Lipofectamine 2000 (Invitrogen) or GeneJuice Transfection Reagent (Merck, Germany) according to manufacturer's instructions. The Rango biosensor was developed in-house according to methods as mentioned in Kalab et. al. [61]. For cold-induced depolymerization assay, cells seeded onto 22mm coverslips were incubated in ice-cold DMEM at 4°C for 1 hour, and proceeded with immunofluorescence as described below.

2.2 Time-lapse Imaging

The effect of temperature shift to non-permissive temperature (39.5°C) on tsBN2 cells or transfected tsBN2 cells expressing Rango, H2B-mCherry, H2B-GFP, tubulin-mCherry, tubulin-GFP, Mst1 WT-mCherry and/or Mst1 K59R-mCherry was followed by time-lapse microscopy. Cells were seeded onto 35mm glass-bottom dishes or Ibidi 8-well chamber slides and placed on a heat-controlled stage of a Zeiss Axiovert 200M microscope. The temperature was maintained at 33.5°C or shifted to 39.5°C and CO₂ levels were maintained at 5% using a CTI 3700 controller (Zeiss, Germany). Phase contrast and fluorescent images were recorded (AxioCam camera and Axiovision 4.6 software) using a 40x objective at every 10 min interval.

2.3 FRET and Image Analysis

With the use of the Rango biosensor, RanGTP levels were deduced via the FRET method. Cells were maintained at 33.5°C or 39.5°C and 5% CO₂ in a heat-controlled chamber on the microscope during FRET experiments. Physiological FRET images were recorded (AxioCam camera and Axiovision FRET 4.6 software) using a 40x objective and FRET analysis was performed using the Axiovision FRET Correction-Youvan Method. The Correction-Youvan method measures the FRET value for an image and performs a 'correction' on the FRET value by deducting any crosstalk from the Donor and Acceptor.

FRET concentration = $(\text{FRET}_{\text{gv}} - \text{bg}_{\text{FRET}}) - \text{Cf}_{\text{don}} * (\text{don}_{\text{gv}} - \text{bg}_{\text{don}}) - \text{Cf}_{\text{acc}} * (\text{acc}_{\text{gv}} - \text{bg}_{\text{acc}})$

(gv = intensity as gray value, bg = background intensity, Cf = correction factor, FRET = FRET image, don = donor image, acc = acceptor image) [67].

2.4 Immunofluorescence Microscopy

Cells seeded onto 22mm coverslips were fixed with 100% ice-cold methanol at -20°C for 10min. After washing thrice with TBST, cells were incubated with primary antibody diluted in TBST (50mM Tris, pH7.6, 150mM NaCl, 0.1% Tween-20) plus 4% bovine serum albumin (BSA; Sigma), at room temperature (RT) for 1.5 hours. Following washes with TBST, the cells were incubated with appropriate secondary antibodies and incubated at RT for 1 hour in the dark. Cells were mounted onto glass slides using ProLong Gold Antifade reagent containing DAPI (Invitrogen).

For immunofluorescence analysis of Crm1 and Mst1, cells were permeabilized with 40µg/ml digitonin in transport buffer (20mM HEPES, 110mM potassium acetate, 5mM sodium acetate, 2mM magnesium acetate, 1mM EGTA, 2mM DTT) at 4°C for 6 min and fixed with 4% paraformaldehyde (PF) in phosphate buffered saline (PBS) for 15 min. After washing thrice with PBS, the cells were stained with antibodies and mounted on glass slides as described above.

For Mst1-mCherry chromosome staining, cells were incubated in hypotonic buffer (75mM KCl) at 37°C for 30 mins before centrifuging onto coverslips at 900rpm for 4 mins in a cytocentrifuge (Cytospin 2, Thermo/Shandon). The cells were first permeabilized with 0.2% Triton X-100 in PBS at RT for 3 min and then fixed with 2% paraformaldehyde in PBS for 10 min. After several washes with PBS, cells were incubated with specific primary antibodies

followed by fluorescent-labeled secondary antibodies and mounted onto glass slides. Images were acquired and analyzed using an Axiovert 200M inverted microscope (Carl Zeiss, Germany) and Axiovision 4.6 software. For immunofluorescence of tubulin, images taken were deconvoluted using the Axiovision 4.6 software.

2.5 Chromosome Spread

Mitotic cells were collected by mechanical shake-off and incubated in hypotonic buffer at 37°C for 20 min. Following hypotonic swelling of the cells, the cells were pelleted by centrifugation at 2000 rpm for 5 min. After that, the cells were washed once and then fixed overnight with ice cold fixative solution (methanol: acetic acid at 3:1) at 4°C. On the following day, the swollen fixed cells were dropped onto slides, dried and stained with ProLong Gold Antifade reagent containing DAPI (Invitrogen). Chromosome spread images were acquired and analyzed using an Axiovert 200M inverted microscope (Carl Zeiss, Germany) and Axiovision 4.6 software.

2.6 Spindle Microtubule Intensity (A.U.) and Relative Fluorescence

Intensity Measurement

Images were acquired with the same exposure time using an Axiovert 200M inverted microscope (Carl Zeiss, Germany) and analyzed with the Axiovision 4.6 software.

Spindle intensity, $SI = (SI_{ave} - CI_{ave}) * SA$, $CI_{ave} = (CI_{total} - SI_{total}) / (CA - SA)$

(CI = cell intensity, CA = cell area, SA = Spindle area)

Relative Aurora B kinase (pThr232) fluorescence intensity = phosphoAurora
B kinase Intensity_{ave}/Total Aurora B kinase Intensity_{ave}
(Centrosome-specific staining was excluded from the measurements.)

2.7 Western Blotting

Mitotic cells were harvested by mechanical shakeoff, washed with PBS and lysed by 2x sample buffer (62.5mM Tris-HCl, pH 6.8, 2% SDS, 25% glycerol, 5% 2-mercaptoethanol, 0.01% bromophenol blue) containing 10% Complete EDTA-free Protease Inhibitor Cocktail (Roche, Switzerland) and 0.1% phosphatase cocktail inhibitor 1 and 2 (Sigma). The mitotic lysate was boiled for 10 min. Equal amounts of protein were resolved on SDS-PAGE and transferred onto nitrocellulose membranes (Biorad laboratories, USA). Membranes were probed with specific primary antibodies diluted in 10% skim milk in TBST at 4°C overnight. Membranes were washed thrice with TBST before incubating with horseradish peroxidase (HRP)-conjugated anti-mouse IgG or anti-rabbit IgG (Invitrogen, USA) or anti-goat IgG secondary antibodies (Santa Cruz Biotechnology, USA). After washing with TBST, immunoreactive proteins were detected by enhanced chemiluminescence reagent (Amersham Biosciences, USA).

2.8 Digitonin permeabilized assay

Hela cells were treated with 10 μ M of MG132 for 4 hours prior to digitonin permeabilization. Cells were then permeabilized with 20 μ g/ml digitonin in transport buffer containing Ran wild-type or Ran mutants, Ran Q69L (dominant positive analog) or RanT24N (dominant negative analog)

(Cytoskeleton Inc., USA), with 10 kDa dextran + FITC for 5 minutes at RT. The cells were rinsed twice with PBS and incubated in DMEM for 1 hour at 37°C before fixing with ice-cold methanol and proceeded with immunofluorescence staining as described.

2.9 Immunoprecipitation

Protein G-sepharose beads (Zymed), specified antibody and cell lysates were incubated at RT for 1 hour. The immunoprecipitates were washed with PBS twice, and then 2x sample buffer was added, boiled at 100°C to denature the proteins, separating them from the beads. Immunoprecipitated protein was analyzed by SDS-PAGE and western blotting.

2.10 RNAi-mediated silencing of Mst1

Stealth select RNAi™ for Mst1 (Invitrogen) was utilized to deplete Mst1 protein level. Mst1 silencing was carried out using 10nM of the oligo (AAU GAU AUC AGA UAC AGA ACC AGC C). RNAi Negative Control Duplexes (Invitrogen, USA) served as negative control in each experimental set. The indicated RNAi were introduced into the cells by transfection using Lipofectamine RNAiMAX (Invitrogen). The transfected cells were harvested after 24 hours and resuspended in 2x SDS sample buffer and boiled. Depletion was assessed by western blotting as described above.

2.11 Immunoprecipitation for kinase assay

24 hours after transfection with Aurora B kinase-GFP, tsBN2 cells were treated with MG132 for 2 hours prior to incubation at permissive or non-

permissive temperature for 4 hours. Then the cells were washed with PBS and lysed in buffer C (20mM HEPES, pH7.5, 10mM KCl, 1.5mM MgCl₂ and 0.5% Nonidet P-40 substitute) containing 10% Complete EDTA-free Protease Inhibitor Cocktail (Roche, Switzerland) and 0.1% phosphatase cocktail inhibitor 1 and 2 (Sigma). Lysates were incubated with protein G-sepharose beads (Zymed) and anti-Aurora B kinase mouse monoclonal antibody (BD Pharmingen) at RT for 1.5 hours. The immunoprecipitates were washed thrice with buffer C and once with buffer D (10mM HEPES, pH7.5, 10mM KCl, 1mM DTT and 10mM MgCl₂). Samples were resuspended in 20µl of kinase mixture (20mM HEPES, pH7.5, 10mM KCl, 1mM DTT, 10mM MgCl₂ and 100µM ATP). 6µg of histone H3 (New England Biolabs) is added to each reaction mixture and reactions were incubated at 30°C for 30 min. The reactions were stopped by incubation on ice and the samples were eluted with 2x sample buffer and analyzed by SDS-PAGE and western blotting.

2.12 Statistical Analysis

Data are presented as \pm standard deviation and analyzed via Student's *t*-test.

P value of < 0.05 is considered statistically significant.

2.13 Antibodies

Antibodies used are summarized in Table 1.

2.14 Plasmids

Plasmids used are summarized in Table 2.

Table 1. Antibodies Used

Primary Antibody	Immunogen	Host/Clonality	Company	Dilutions		Amount (µg)
				WB	IF	IP
RCC1 : (N-19)	Epitope mapping at the N-terminus of human RCC1	Goat/Polyclonal	Santa Cruz Biotechnology, USA	1:1000	-	-
Ran : (C-20)	Epitope mapping at the C-terminus of human Ran	Goat/Polyclonal	Santa Cruz Biotechnology, USA	1:1000	-	-
RanGAP1 : (H-180)	Human RanGAP1 aa 408-587	Rabbit/Polyclonal	Santa Cruz Biotechnology, USA	1:1000	1:500	-
RanBP1 : (C-19)	Peptide mapping C-terminus of human RanBP1	Goat/Polyclonal	Santa Cruz Biotechnology, USA	1:1000	-	-
GFP : (B-2)	Full length GFP of Aequorea victoria origin	Mouse/Monoclonal	Santa Cruz Biotechnology, USA	1:1000	-	-
Mst1 : (EP1465Y)	Synthetic peptide corresponding to residues near the N-terminus of human Mst1	Rabbit/Monoclonal	Genetex Inc., USA	-	1:500	-
Mst1 : (N-terminal)	Synthetic peptide corresponding to residues near the N-terminus of human Mst1	Rabbit/Polyclonal	Cell Signaling, USA	1:1000	-	-
Crm1 : (N-terminal)	Human Crm1 aa 2-122	Mouse/Monoclonal	BD Pharmigen, USA	1:1000	-	-

Crm1 : (H-300)	Human Crm1 aa 772-1071	Rabbit/Polyclonal	Santa Cruz Biotechnology, USA	-	1:500	-
Phospho Histone H3(Ser10)	Synthetic phosphopeptide corresponding to residues surrounding Ser10 of human histone H3	Rabbit/Polyclonal	Cell Signaling, USA	1:1000		-
Actin : (C-11)	C-terminus of human actin	Goat/Polyclonal	Santa Cruz Biotechnology, USA	1:1000		-
Hec-1	Human Hec-1 aa 495-608	Mouse/Monoclonal	BD Pharmigen, USA	-	1:1000	-
BubR1	Human BubR1 aa 276-388	Mouse/Monoclonal	BD Pharmigen, USA	-	1:1000	-
TPX2 : (H-300)	Human TPX2 aa 448-747	Rabbit/Polyclonal	Santa Cruz Biotechnology, USA	-	1:1000	-
Dynactin p150	Rat p150 aa 2-303	Mouse/Monoclonal	BD Pharmigen, USA	1:1000	1:1000	-
Securin : (DCS 280)	Recombinant full length human securin	Mouse/Monoclonal	Abcam, UK	1:1000		-
Centromeric Antigens	Centromeric proteins	Human/Polyclonal	Antibodies Incorporated, USA	-	1:10	-
Phospho cdk1 (Thr161)	Synthetic phosphopeptide corresponding to residues surrounding Thr161 of human cdk1	Rabbit/Polyclonal	Cell Signaling, USA	1:1000	-	-
Aurora B kinase : (N-terminal)	Rat Aurora B kinase aa 2-124	Mouse/Monoclonal	BD Pharmigen, USA	1:1000	1:1000	32
Phospho-Aurora A	Synthetic peptide corresponding to	Rabbit/Monoclonal	Cell Signaling, USA	1:1000	1:500	-

(Thr288)/Aurora B (Thr232)/Aurora C (Thr198) : (D13A11)	residues surrounding Thr232 of Aurora B kinase					
DsRed	Antisera raised against DsRed-Express, a variant of <i>Discosoma</i> sp. red fluorescent protein.	Rabbit/Polyclonal	Clontech Laboratories, Inc., USA	1:1000	-	-
α -tubulin clone DM1 α FITC-conjugate	Carboxyl-terminal of α -tubulin	Mouse/Monoclonal	Sigma Aldrich, USA	-	1:1000	-
FLAG : (M2)	FLAG sequence at the N-terminus, Met-N-terminus or C-terminus of FLAG fusion proteins	Mouse/Monoclonal	Sigma Aldrich, USA	-	-	14
Secondary Antibody	Immunogen	Host	Company	Dilutions		
				WB	IF	IP
Alexa Flour 488 anti-rabbit IgG	Rabbit IgG heavy and light chains	Goat	Invitrogen, USA	-	1:500	-
Alexa Flour 594 anti-rabbit IgG	Rabbit IgG heavy and light chains	Goat	Invitrogen, USA	-	1:500	-
Alexa Flour 488 anti-mouse IgG	Mouse IgG heavy and light chains	Goat	Invitrogen, USA	-	1:500	-
Alexa Flour 594 anti-mouse IgG	Mouse IgG heavy and light chains	Goat	Invitrogen, USA	-	1:500	-
Rhodamine		Donkey	Jackson	-	1:50	-

Red-X conjugate anti-human IgG			Immunoresearch - Laboratories, USA			
Rabbit IgG HRP conjugate	Rabbit IgG heavy and light chains	Goat	Invitrogen, USA	1:10 000	-	-
Goat IgG HRP conjugate	Goat IgG heavy and light chains	Rabbit	Invitrogen, USA	1:10 000	-	-
Mouse IgG HRP conjugate	Mouse IgG heavy and light chains	Goat	Santa Cruz Biotechnology, USA	1:10 000	-	-

Abbreviations: IF, immunofluorescence; WB, western blot; IP, immunoprecipitation; aa, amino acid.

Table 2. Plasmids Used

Plasmid	Figure
H2B-GFP	3.3.1, 3.6.2, 3.9.1
H2B-mCherry	3.2.2A
Tubulin-mCherry	3.2.2B, 3.3.1, 3.3.3, 3.6.2
Wild-type (WT) RCC1-GFP	3.3.3
Rango	3.1, 3.2.2, 3.2.3
Mst1 WT-mCherry	3.9.1
Mst1 K59R-mCherry	3.9.1
Mst1 K59R Δ C-mCherry	3.10.3
mCherry	3.9.1
FLAG-Mst1 WT	3.10.1, 3.10.2
FLAG-Mst1 K59R	3.10.1, 3.10.2
FLAG-Mst1 K59R Δ C	3.10.1, 3.10.2
FLAG	3.10.1, 3.10.2
Aurora B kinase-GFP	3.5.2, 3.10.1, 3.10.2

Chapter 3 : Results

3.1 Rango as a GTP indicator

Although the presence and importance of the RanGTP gradient during mitosis has been demonstrated via computational models, biosensors and associated *in vitro* and *in vivo* studies in mammalian cell lines, the precise mechanistic pathways by which RanGTP exerts its regulatory roles throughout mitosis have yet to be thoroughly deconstructed [27,68,69,70]. Therefore, I sought to establish a system, which would allow direct visualization of real time changes in the RanGTP gradient by time-lapse imaging. To this end, the temperature sensitive tsBN2 cells was chosen due to its mutation in the RCC1 gene, whereby incubation at non-permissive temperature (39.5°C) leads to depletion of RCC1 protein and RanGTP subsequently [71]. As a measure of RanGTP level, the Rango biosensor was selected [61]. Prior to performing the time-lapse proper, I sought to examine the utility of the chosen biosensor and cell line. Combining the acceptor-photobleaching method and confocal microscopy, I was able to observe increase in donor CFP FRET intensity when acceptor YFP was photobleached. This increase in donor CFP FRET was significantly lower in temperature-shifted tsBN2 cell incubated at non-permissive temperature (Fig.3.1A). Control cells incubated at permissive temperature showed 20.4% FRET efficiency compared to 11.1% FRET efficiency in temperature-shifted cells incubated at non-permissive temperature (Fig. 3.1B). The lower FRET efficiency in temperature-shifted cells indicated that RCC1 has been depleted and that the Rango biosensor can be used in tsBN2 cells to report levels of RanGTP.

Although the acceptor-photobleaching method was able to ascertain the utility of the Rango biosensor for our study, due to the photobleaching effect of the technique, it was not possible to obtain direct visualization of the changes in the RanGTP levels or perform live cell time-lapse imaging with this method. Therefore, subsequent Rango-mediated experiments were performed using the Axiovision FRET Correction-Youvan Method (as described in Materials and Methods). The distribution of RanGTP, as indicated by Rango FRET signal, from prometaphase to late anaphase is shown in Fig. 3.1C. A high RanGTP level is present surrounding the chromosomes and it progressively declines towards the periphery. Meanwhile, during anaphase, there is a high RanGTP level at the midbody whereby the concentration of RanGTP is crucial for the spatial recruitment of the plethora of proteins involved in NE reformation and cytokinesis.

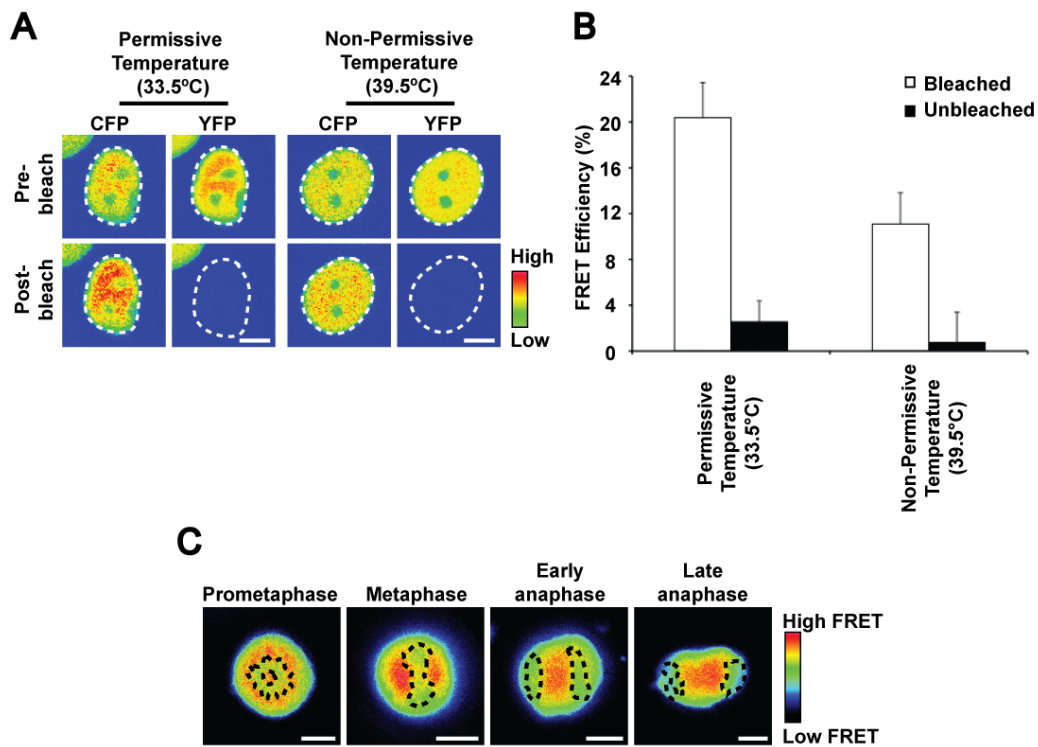


Figure 3.1: FRET biosensor, Rango, as a RanGTP indicator.

A) FRET signal shows presence of RanGTP in interphase nuclei. tsBN2 cells were incubated at permissive (33.5°C) or non-permissive temperature (39.5°C) for 3 hours before FRET. Images of interphase nuclei in CFP and YFP pre- and post-photobleaching are shown. White dashed lines outline the nuclei. B) The increase in FRET efficiency was significantly higher for cells incubated at permissive temperature as compared to those incubated at non-permissive temperature. Changes in CFP intensity after photobleaching (white columns) was compared to CFP intensity fluctuations in control unbleached interphase nuclei (black columns). Error bars represent \pm standard deviation (s.d.). ($p < 0.001$, Student's t test, $n = 30$) C) Distribution of FRET tsBN2 cells from prometaphase to late anaphase. Black dashed lines outline the chromosomes. Color bar represents FRET intensity. Scale bar: 10 μm .

3.2 High RanGTP is important for the maintenance of proper chromosome alignment at the metaphase plate

Considering that the RanGTP gradient is most obvious during metaphases and accumulates maximally around metaphase chromosomes, tsBN2 cells were arrested at metaphase using MG132 for 2 hours, prior to incubation at permissive (control) or non-permissive temperature (Fig. 3.2.1).

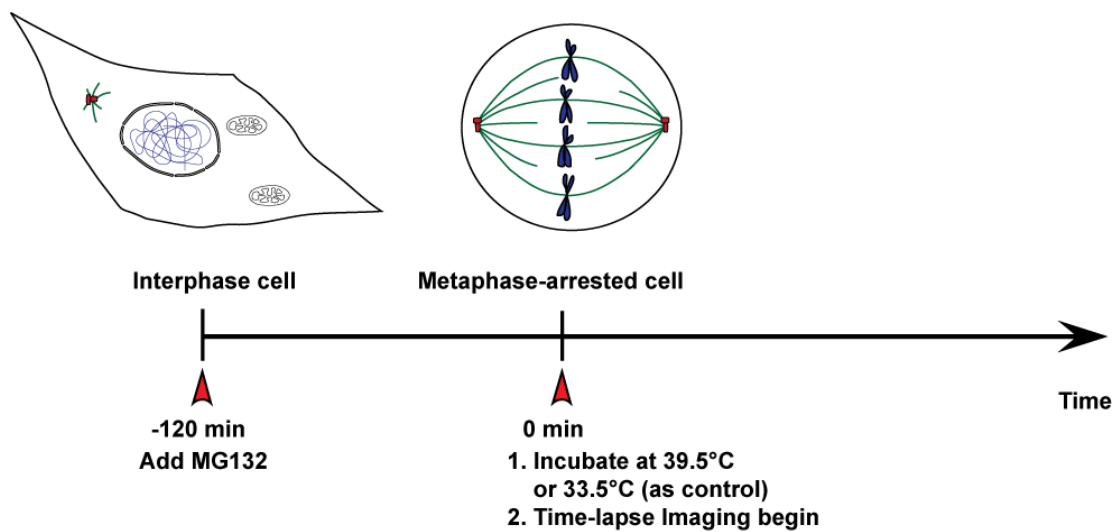


Figure 3.2.1: Schematic depiction of the experimental conditions. Cells were arrested at metaphase using MG132 for 2 hours, prior to incubation at permissive or non-permissive temperature for subsequent imaging or biochemical analysis.

Time-lapse imaging using tsBN2 cells co-transfected with either Rango and H2B-mCherry (Fig. 3.2.2A) or Rango and tubulin-mCherry (Fig. 3.2.2B) were performed. The FRET intensity for both the controls (Fig. 3.2.2A and 3.2.2B, color encoding images) remain evenly high surrounding the metaphase chromosome; whereas for the temperature-shifted cells, the FRET intensity declined as the time-lapse progressed (Fig. 3.2.2A and 3.2.2B, color encoding images). Quantification of the relative FRET intensity for control and temperature-shifted cells are shown in Fig. 3.2.2C; the relative FRET intensity for control cells stabilizes around 1.0 while the value for

temperature-shifted cells progressively decreased to about 0.8 after 3 hours. To the best of my knowledge, no existing reports have been found to depict the real time collapse of the RanGTP gradient in tsBN2 cells.

Whilst the decline in FRET intensity was an expected phenotype, it was of interest to observe that chromosome misalignment occurred in the temperature-shifted cells (Fig. 3.2.2A, lower panel). Control cells exhibited normal metaphase chromosome alignment throughout the time-lapse imaging (Fig. 3.2.2A, upper panel). This chromosome misalignment phenotype was unexpected considering that the cells had already achieved stable kinetochore-microtubule attachments for proper chromosome alignment at the metaphase plate as they were arrested at metaphase prior to incubation at the non-permissive temperature. With further analysis, the possibility that the observed phenotype was due to compromised mitotic spindles upon temperature change was ruled out. This is because, as shown by the mCherry-tagged tubulin in Fig. 3.2.2B, the metaphase spindle remained intact throughout the time-lapse despite the increase in temperature.

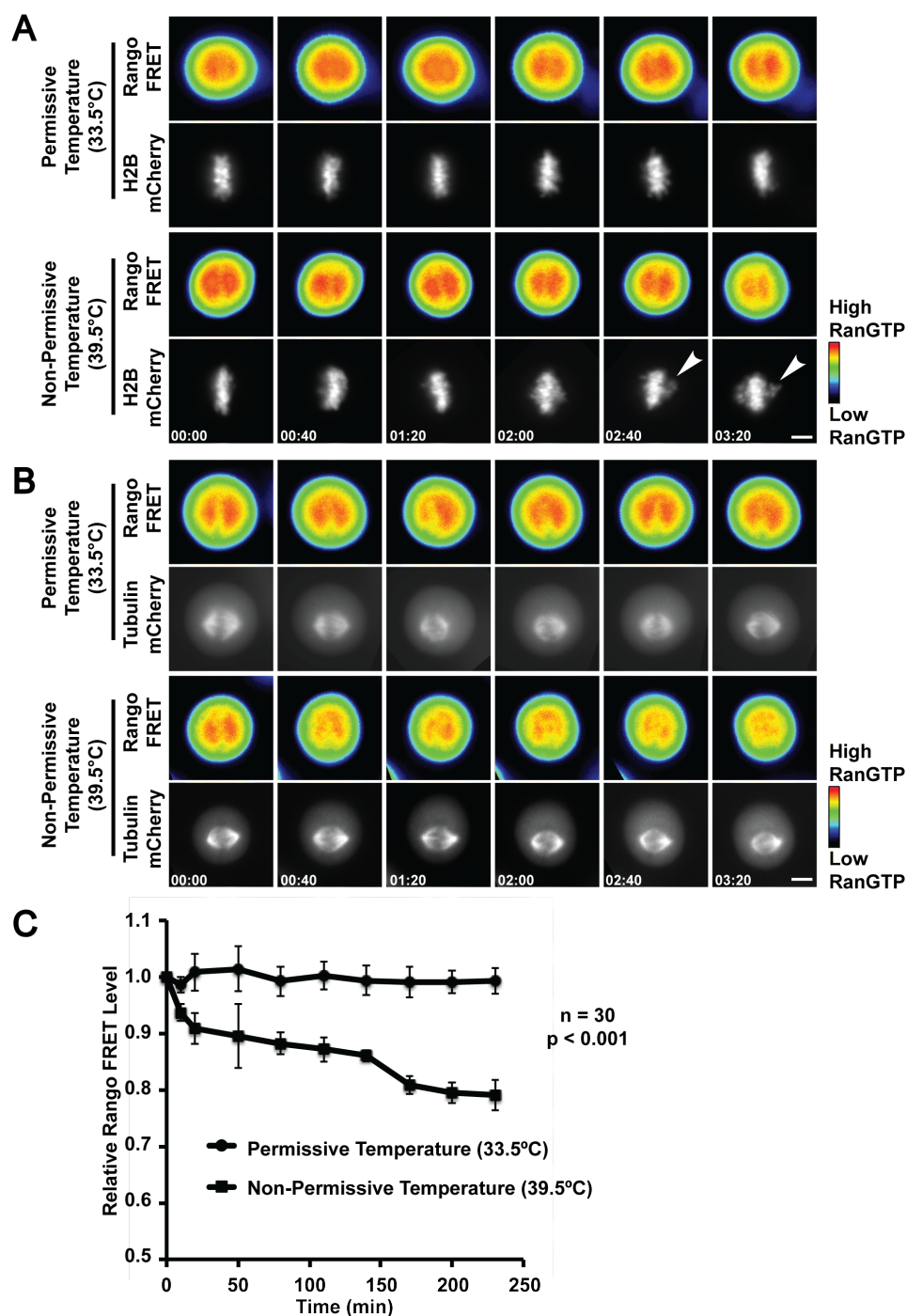


Figure 3.2.2: Incubation of tsBN2 cells at non-permissive temperature causes decline in RanGTP levels and compromises the maintenance of metaphase chromosome alignment.

A) tsBN2 cells expressing Rango and H2B-mCherry. Chromosomes displaced from the metaphase plate are indicated by the arrowheads. B) tsBN2 cells expressing Rango and tubulin-mCherry. Control experiments at permissive temperature (upper panel) and temperature-shift experiments at non-permissive temperature (lower panel). Color bar represents FRET intensity. Scale bar: 10 μ m. C) Line chart representation of relative FRET intensity (according to Youvan's method) at various time-lapse intervals for control (round markers), and temperature-shifted (square markers) cells.

Error bars represent \pm s.d. from three independent experiments. ($p < 0.001$, Student's t test).

In order to ascertain that the observed change in FRET intensity for temperature-shifted cells was not attributed to degradation of the Rango probe or changes in Ran levels upon increase in temperature, levels of both the Rango and Ran proteins were probed. Both protein levels remained consistent for both control and temperature-shifted cell lysates (Fig. 3.2.3). This indicates that the Rango biosensor remained intact despite the increase in temperature and any changes in FRET intensities should be due to variations in RanGTP levels. Therefore, the data suggests that high RanGTP is key to the maintenance of proper chromosome alignment during metaphase.

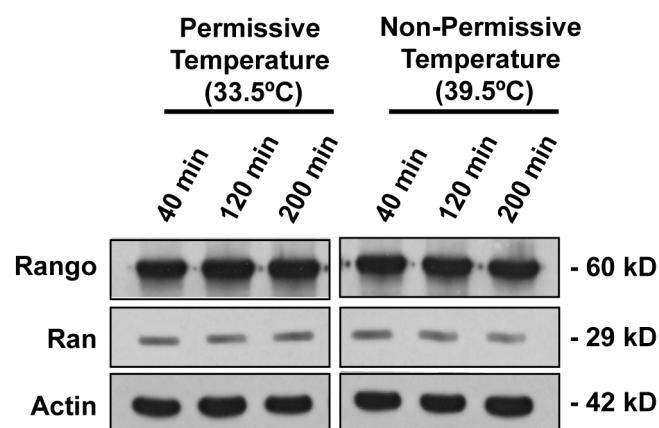


Figure 3.2.3: FRET biosensor Rango and Ran protein levels remain stable at non-permissive temperature.

Western blot analysis of Rango and Ran from mitotic cells incubated at permissive or non-permissive temperature for various time points. Actin was used as loading control.

3.3 RCC1 depletion causes misalignment of metaphase chromosome

Although the Rango biosensor is widely used in RanGTP studies, the overabundance of the importin- β binding (IBB) domain can potentially generate an “importin- β sink” effect and thus affecting downstream processes. Therefore, it was imperative to conduct a subsequent experiment without overexpression of Rango, to ensure that the chromosome misalignment phenotype is not attributed to overexpression of Rango and thus exclude this possibility. To this end, live cell imaging was conducted on cells co-transfected with H2B-GFP and tubulin-mCherry, in the absence of Rango. Results showed that temperature-shifted metaphase cells exhibited similar chromosome misalignment phenotype, as depicted by the H2B-GFP images of chromosomes displaced from the metaphase plate. As the time-lapse progressed, more chromosomes appeared to have escaped from the metaphase plate. In addition, it was important to note that although gross chromosome misalignment was observed, the metaphase spindle remained intact and unperturbed by the temperature change (Fig. 3.3.1A, lower panel). Meanwhile, control metaphase cells incubated at permissive temperature continued to display properly aligned chromosomes at the metaphase plate throughout the time-lapse (Fig. 3.3.1A, upper panel). Quantification of at least 30 metaphase cells each from time-lapse imaging indicated that a significant proportion of temperature-shifted metaphase cells exhibited chromosome misalignment (Fig. 3.3.1B).

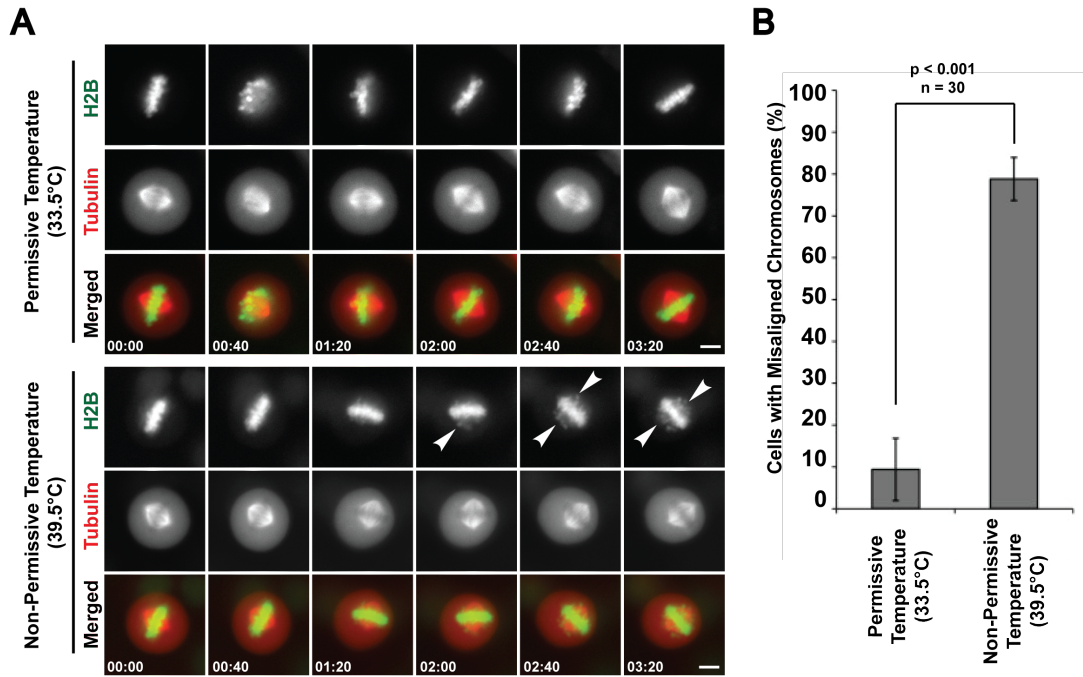


Figure 3.3.1: RCC1 depletion at non-permissive temperature causes misalignment of metaphase chromosome without affecting spindle structure.

A) Time-lapse imaging of tsBN2 cells expressing H2B-GFP and tubulin-mCherry. Control experiment at permissive (upper row) and temperature-shift experiment at non-permissive temperature (lower row). Chromosomes displaced from the metaphase plate are indicated by the arrowheads. B) Histogram shows percentage of time-lapse imaged cells with misaligned chromosomes. Error bars show \pm s.d. from three independent experiments. ($p < 0.001$, Student's *t* test).

Immunoblotting analysis was performed on mitotic cell lysates harvested at various time points after incubation at permissive or non-permissive temperature and probed with antibodies as indicated in Fig. 3.3.2. As predicted, temperature-shifted cell lysates showed prominent decline in RCC1 protein levels. Meanwhile, protein levels of Ran regulators, RanGAP1 and RanBP1, did not show significant differences between both control and temperature-shifted cell lysates. Therefore, it can be conclude that the changes observed should be attributed to the loss of RCC1 alone upon increase in temperature.

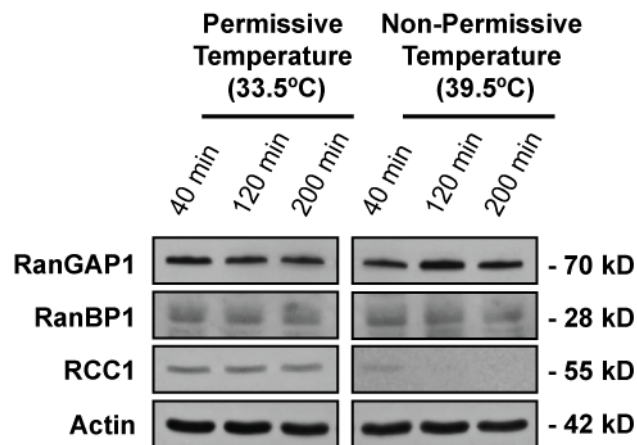


Figure 3.3.2: RCC1 is efficiently depleted at non-permissive temperature.

Western blot analysis of mitotic tsBN2 cell incubated at permissive or non-permissive temperature and harvested via mechanical shake-off at various time points. Actin was used as loading control.

If RCC1 depletion was indeed responsible for the observed chromosome misalignment phenotype, complementation with functional wild-type (WT) RCC1 protein should circumvent the aberrant chromosome alignment even when the metaphase cells are incubated at non-permissive temperature. Therefore, GFP-tagged WT- RCC1 was expressed in tsBN2 cells and the time-lapse imaging experiment was repeated at non-permissive temperature. In accordance, the misalignment phenotype was rescued by the presence of WT-RCC1 protein (Fig. 3.3.3A), thus reaffirming that the loss of RCC1 caused the misalignment of metaphase chromosomes. Quantification of at least 30 cells each from time-lapse imaging showed that the expression of WT-RCC1 significantly reduced the proportion of affected cells (Fig. 3.3.3B). Further immunoblotting of RCC1 and GFP protein levels also showed that the overexpressed WT-RCC1 protein was sufficient and necessary to compensate for the loss of endogenous RCC1 protein in tsBN2 cells upon increase in temperature (Fig. 3.3.3C). Hence, these results confirm that the phenotype observed can be attributed to the loss of RCC1 protein, and its corresponding collapse of the mitotic RanGTP gradient.

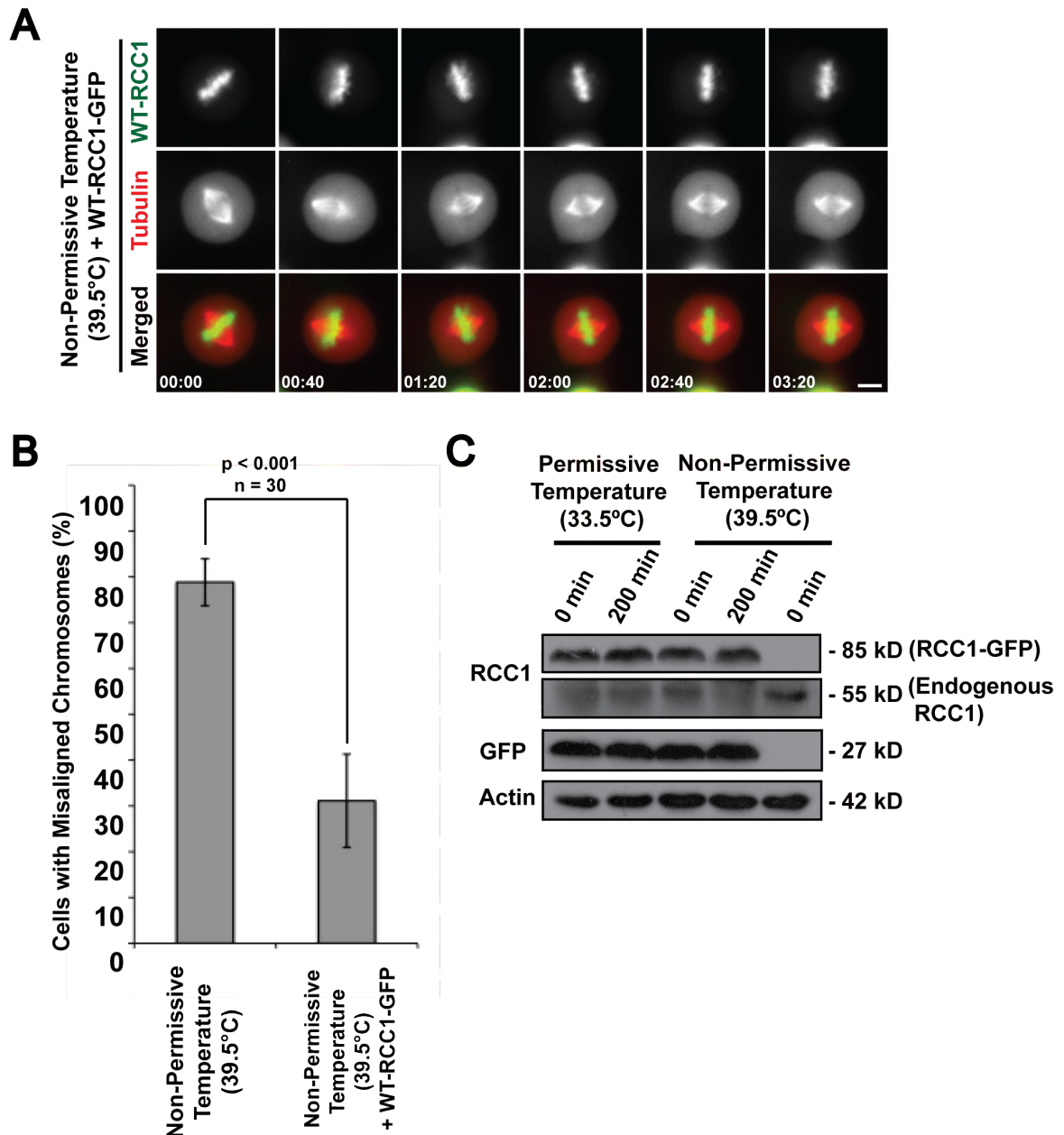


Figure 3.3.3: Complementation with wild-type RCC1 reinstated proper metaphase chromosome alignment at non-permissive temperature.

A) Time-lapse imaging of tsBN2 cells expressing wild-type RCC1-GFP and tubulin-mCherry. Experimental conditions for time-lapse imaging and the parallel western blotting were conducted as shown in Fig. 3.2.1. Expression of wild-type RCC1-GFP in tsBN2 cells incubated at non-permissive temperature abrogated the misalignment phenotype. Scale bar: 10 μ m. B) Histogram shows percentage of time-lapse imaged cells with misaligned chromosomes. Error bars show \pm s.d. from three independent experiments. ($p < 0.001$, Student's t test). C) Western blot analysis of mitotic tsBN2 cells incubated at permissive or non-permissive temperature and harvested via mechanical shake-off at various time points. Lanes 1-4 represent samples transfected with wild-type RCC1-GFP. Lane 5 represents control samples without wild-type RCC1-GFP transfection. Actin was used as loading control.

To further confirm that the state of Ran is imperative to the maintenance of proper chromosome alignment, recombinant Ran protein and its mutants were incubated with digitonin-treated HeLa cells bearing functional *RCC1* gene. Results indicated that cells incubated with Ran T24N (dominant negative, non-phosphorylatable analog) were more susceptible to aberrant chromosome displacement from the metaphase plate as compared to cells incubated with Ran wild-type, Ran Q69L (dominant positive, non hydrolyzable analog) or with control FITC-dextran only (Fig. 3.3.4C). This result indicates that perturbation to Ran's nucleotide state affects its functionality and that active RanGTP is required to regulate the stability of kinetochore-microtubule attachments. Therefore providing direct evidence to RanGTP's involvement in the preservation of the alignment of metaphase chromosomes at the equator.

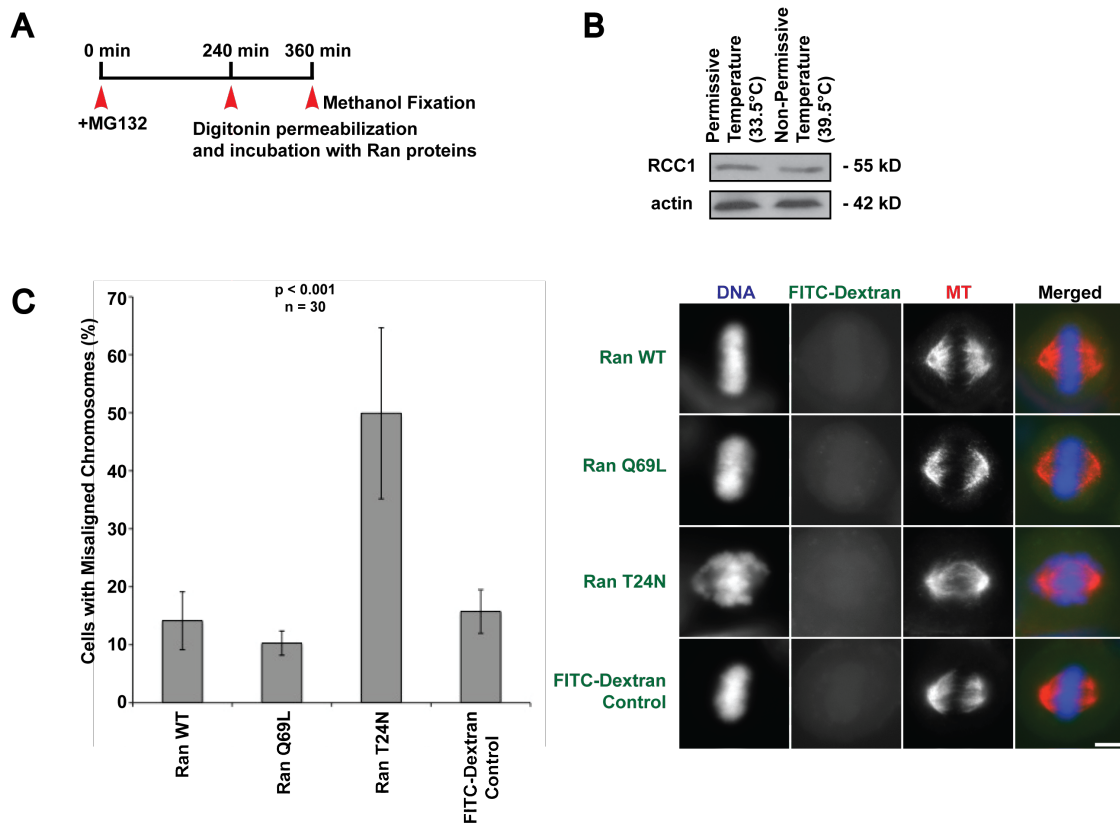


Figure 3.3.4: Functionally active RanGTP is crucial for stable chromosome alignment at metaphase.

A) Schematic depiction of experimental conditions. Cells were arrested at metaphase with 10 μ M of MG132 for 4 hours, prior to permeabilization with digitonin and incubation with Ran proteins. Cells were then incubated with Ran proteins for 1 hour at 37°C and fixed with ice-cold methanol. B) Western blot analysis of mitotic HeLa cells incubated at permissive or non-permissive temperature and probed with RCC1 antibody. RCC1 protein was not degraded at non-permissive temperature. Actin was used as loading control. C) Histogram shows percentage of metaphase cells with misaligned chromosomes. Error bars show \pm s.d. from three independent experiments. ($p < 0.001$, One way ANOVA). D) Representative images of the majority population of metaphase cells incubated with Ran proteins as indicated. Scale bar: 10 μ m.

3.4 RanGTP regulates the stability of kinetochore-microtubule attachments and prevents reactivation of the spindle assembly checkpoint prior to anaphase entry

Meanwhile, it was imperative to clarify that the observed chromosome misalignment phenotype was not due to reversal to prometaphase or a manifestation of premature anaphase onset due to slippage of SAC arrest. Immunoblotting of levels of cyclin A indicated that the protein level of cyclin A remained consistent throughout the time points without any increase which suggests G2 phase reentry, thus eliminating the likelihood of reversal to prometaphase. Immunoblotting of levels of cyclin B1 and phosphorylated cdk1 (Thr161) showed no significant change for both control and temperature-shifted cells, indicating that the APC is still inhibited and that the cells were arrested at metaphase. Also, protein levels of SMC1 and securin did not show any decline, indicative of intact cohesion complex and securin (Fig. 3.4.1.A). In addition, phosphorylated histone H3 (Ser10) characteristic of anaphase onset did not show any decline. A further examination of the chromosome spread of temperature-shifted cells showed condensed chromosomes consisting of two intact sister chromatids, which is characteristic of metaphasic chromosomes (Fig. 3.4.1.B). These results thus reaffirms that the observed phenotype occurs at metaphase without reversal to prometaphase or premature anaphase onset.

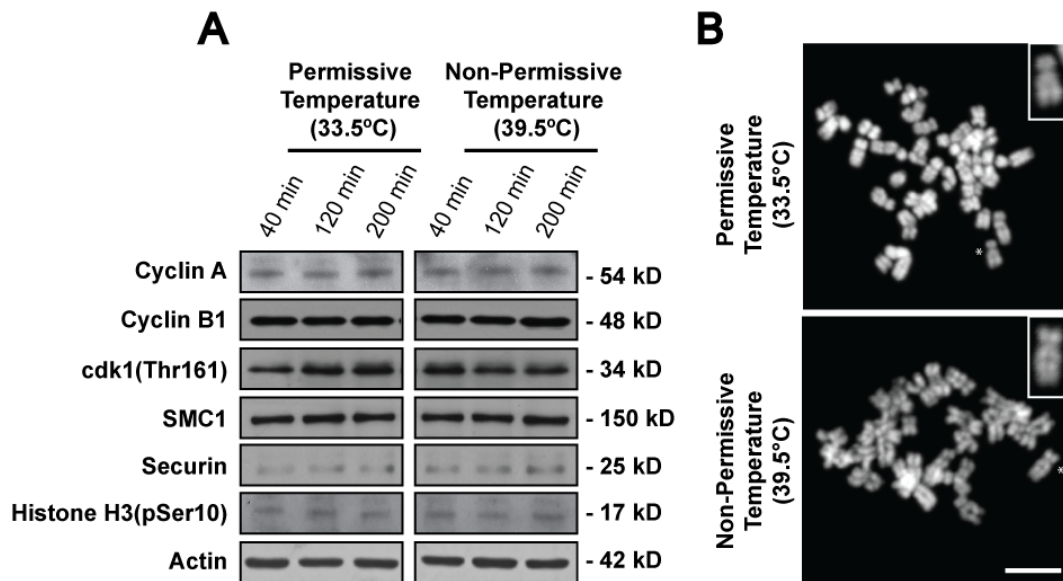


Figure 3.4.1: Aberrantly aligned chromosomes are composed of metaphase chromosomes with intact sister chromatids.

A) Western blot analysis of mitotic tsBN2 cells incubated at permissive or non-permissive temperature and harvested via mechanical shake-off at various time points. Actin was used as loading control. B) Chromosome spread of mitotic tsBN2 cells incubated at permissive or non-permissive temperature. Magnified image of metaphase chromosome marked with asterisks (*) is shown inset, depicting tightly condensed metaphase chromosome with intact sister chromatids. Scale bar: 10 μ m.

Upon establishing that the observed phenotype occurs at metaphase, aberrant chromosome displacement from the metaphase plate could be due to either erroneous kinetochore-microtubule attachments or loss of attachments to spindle microtubules, as mentioned in the introduction. In order to address these possibilities, metaphase cells incubated at permissive or non-permissive temperature were immunostained with anti-centromeric antigens (ACA) and anti-tubulin antibodies. Both control and temperature-shifted metaphase cells displayed localization of ACA on chromosomes at the metaphase plate, and for temperature-shifted cells, localization of ACA was observed on chromosomes escaped from the metaphase plate as well (Fig. 3.4.2A). Whilst magnified images on the right showed proper ACA-

microtubule attachment in control cells (Fig. 3.4.2.A, upper panel), such attachments were compromised in the temperature-shifted cells (Fig. 3.4.2.A, lower panel).

Stable kinetochore-microtubule attachments render spindle microtubules resistance towards cold exposure while unattached microtubules are susceptible to low temperature-induced depolymerization [39,72]. To further substantiate the aforementioned data, control and temperature-shifted cells were subjected to cold-induced depolymerization for ensuing immunocytochemistry analysis. Quantified relative signal intensities of spindle microtubules revealed that the proportion of cold-stable microtubules was significantly lower in cells subjected to non-permissive temperature as compared to control cells (Fig. 3.4.2.B and C). These results indicate that the misaligned chromosomes have lost proper, end-on, bipolar attachments upon RanGTP depletion.

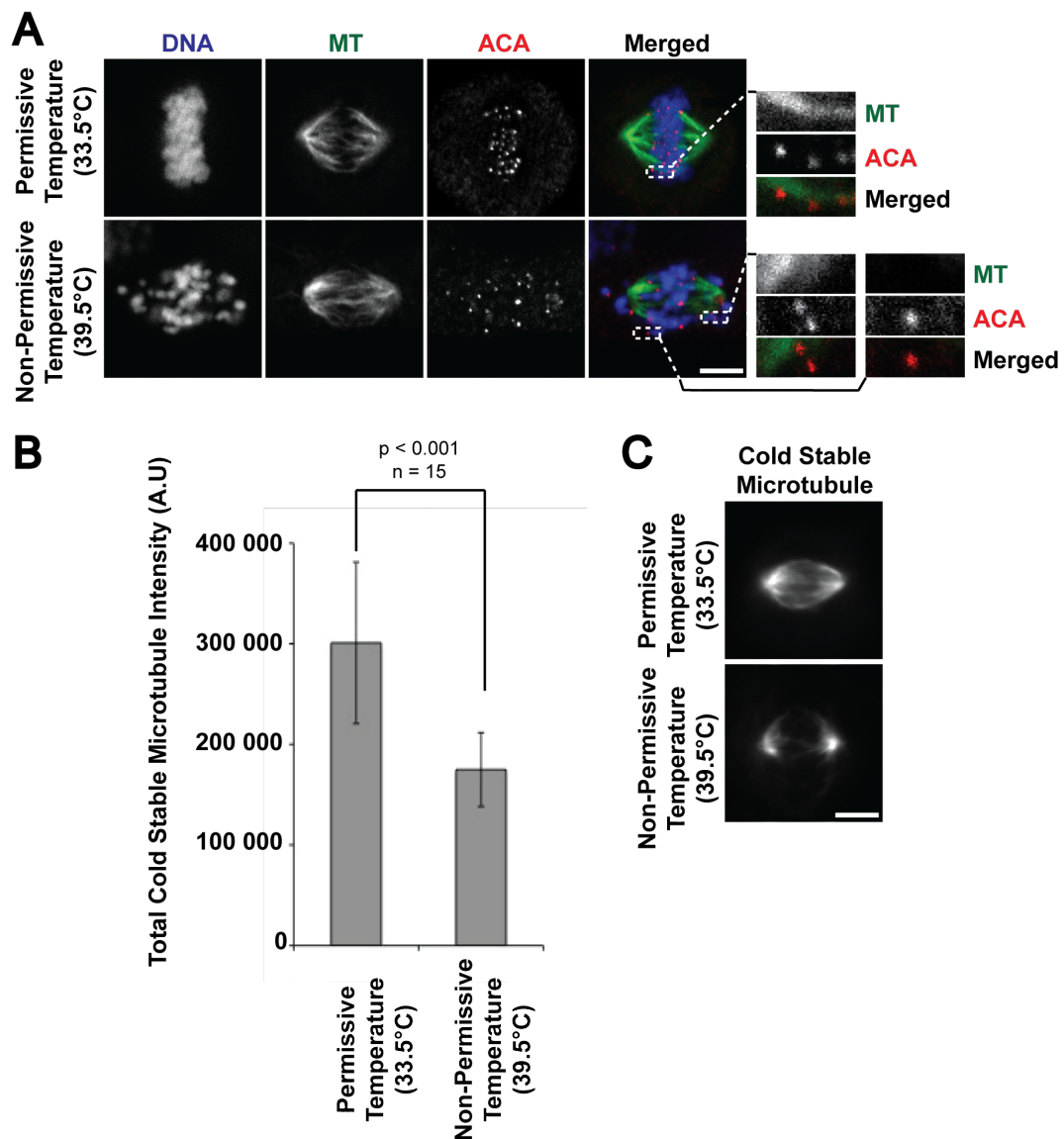


Figure 3.4.2: Mitotic RanGTP is required for stable attachment of microtubules to the kinetochores.

A) Cells were immunostained with anti-centromere antigens (ACA) and tubulin antibodies. Magnified images show end-on kinetochore-microtubule attachment (control, upper panel) and unattached chromosomes (temperature-shifted, lower panel). Magnified merged image is exclusive of DNA. B) Histogram shows total cold stable microtubule intensity (A.U.) after cold-induced microtubule depolymerization. Error bars show \pm s.d. from three independent experiments. ($p < 0.001$, Student's *t* test). C) Representative images of cold-treated mitotic spindles from cells incubated at permissive or non-permissive temperature. Scale bar: 10 μ m.

As the SAC is an active signal generated by unattached or improperly attached kinetochores, absence of or failure to achieve amphitelic kinetochore-microtubule attachments would result in persisted checkpoint complex localization [73,74]. Consistent with this, control metaphase cells immunostained with anti-BubR1 showed little or no BubR1 at the kinetochores. Meanwhile, temperature-shifted metaphase cells showed distinctive presence of BubR1 at the kinetochores of chromosomes that have escaped from the metaphase plate and to a lesser extent also on chromosomes that remained at the equator (Fig. 3.4.3A). Co-immunostaining with ACA confirmed that the re-assembly of the spindle checkpoint components occurred within the vicinity of the chromosomal centromeric regions (Fig. 3.4.3B). Taken together, this data shows that the mitotic RanGTP is important in governing proper kinetochore-microtubule attachments and thus limiting reactivation of the SAC.

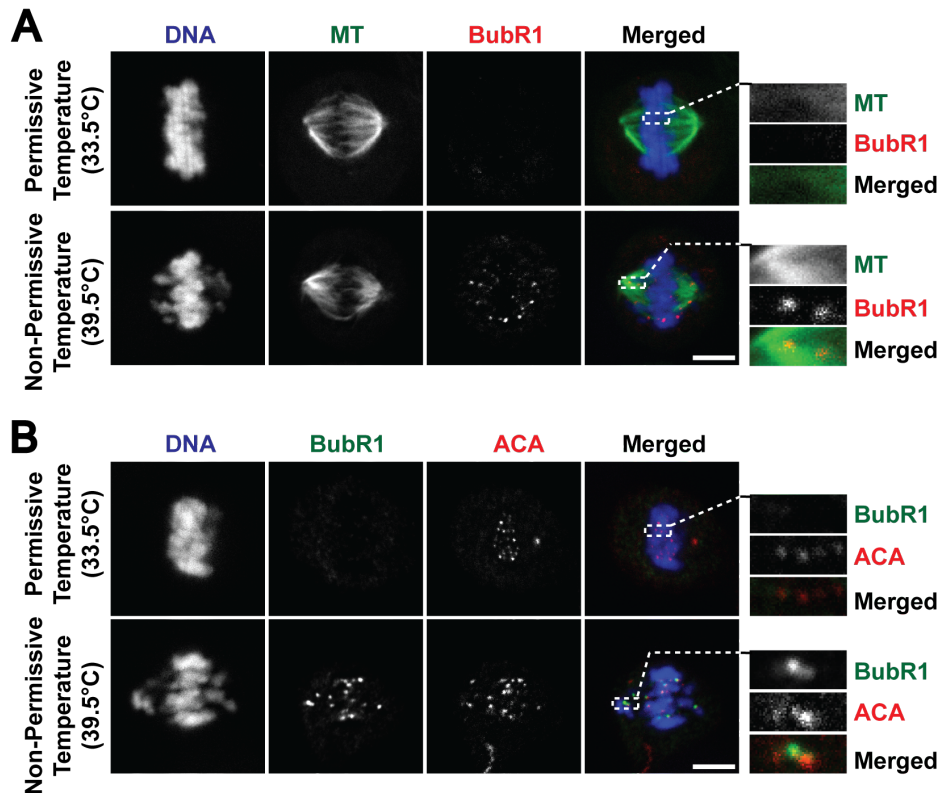


Figure 3.4.3: Mitotic RanGTP is necessary to prevent untimely reactivation of the spindle assembly checkpoint.

Immunostaining of spindle checkpoint protein, BubR1 with A) tubulin or B) centromeric ACA. Magnified merged image is exclusive of DNA. Scale bar: 10 μm .

3.5 Aurora B kinase activity is elevated in RanGTP-depleted cells

Aurora B kinase has been shown to promote depolymerization and reorganization of kinetochore-microtubule attachments [47]. Also, noting its role as a tension sensor and regulator of proper kinetochore-microtubule attachments, it was befitting to consider whether it is involved in the presentation of the chromosome misalignment induced by RanGTP depletion. As an indication of kinase activity, phosphorylation of Aurora B kinase at Thr232 was examined [75]. Immunostaining for active Aurora B kinase showed a more distinct presence of phosphorylated Aurora B kinase at the kinetochores of temperature-shifted metaphase cells (Fig. 3.5.1A). Subsequent quantitative analysis indicated that the ratio of relative fluorescence intensity of phosphorylated to total Aurora B kinase was approximately 1.7 times higher in temperature-shifted metaphase cells (Fig. 3.5.1B). Correspondingly, immunoblotting for active Aurora B kinase revealed that the protein level of active Aurora B kinase is almost double for mitotic cells incubated at non-permissive temperature as compared to the control mitotic cells (Fig. 3.5.1C and D).

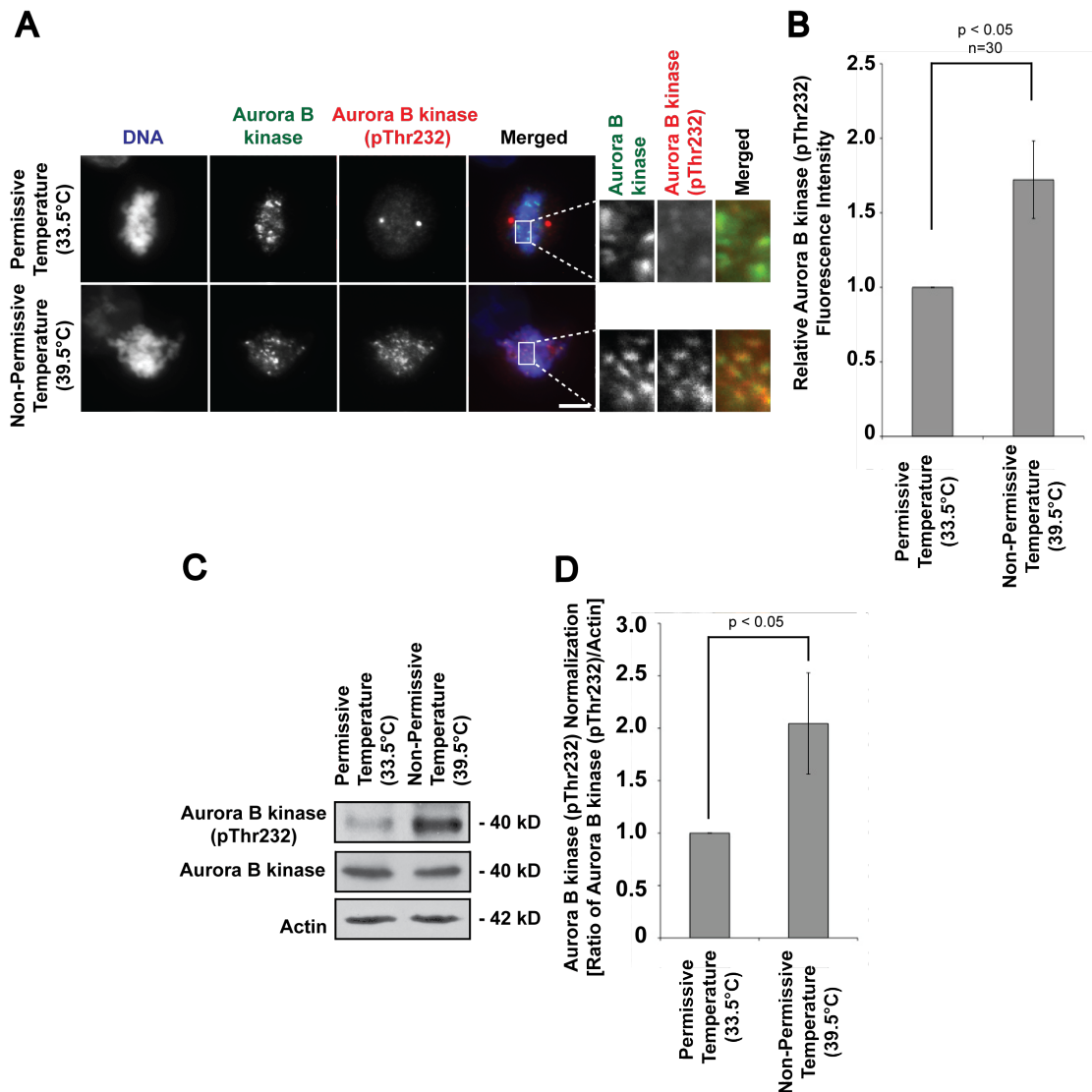


Figure 3.5.1: Active Aurora B kinase phosphorylation at Thr232 after RanGTP depletion.

A) tsBN2 cells incubated at permissive or non-permissive temperature were analyzed by immunofluorescence staining with anti-Aurora B kinase and anti-Aurora B kinase (pThr232). Magnified images are shown on the right. Magnified merged image is exclusive of DNA. Scale bar: 10 μ m. B) Histogram depicting quantification of relative Aurora B kinase (pThr232) fluorescence intensity normalized against total Aurora B kinase fluorescence intensity as mean \pm s.d. from 3 independent experiment (n=30). Images were acquired with fixed exposure time. ($p < 0.05$, Student's t test). C) Western blot analysis of tsBN2 cells incubated at permissive or non-permissive temperature for 4 hours and harvested via mechanical shake-off. Actin was used as loading control. D) Quantified Aurora B kinase (pThr232) intensities were normalized and presented as relative fold change \pm s.d. (error bar) of three independent experiments. ($p < 0.05$, Student's t test).

In order to ascertain that the kinase activity of Aurora B kinase is increased in the temperature-shifted cells, an *in vitro* kinase assay on recombinant Histone H3 was conducted with immunoprecipitated Aurora B kinase from mitotic cells incubated at permissive or non-permissive temperature. Kinase activity was determined based on phosphorylation of Histone H3, which is a known substrate of Aurora B kinase. Results showed that there was significantly higher level of phosphorylated histone H3 (Ser10), thus indicating that kinase activity of Aurora B kinase was indeed elevated in temperature-shifted cells (Fig. 3.5.2A and B). Notably, these results suggest a possible link between Aurora B kinase and the manifestation of aberrant chromosome alignment upon RanGTP depletion.

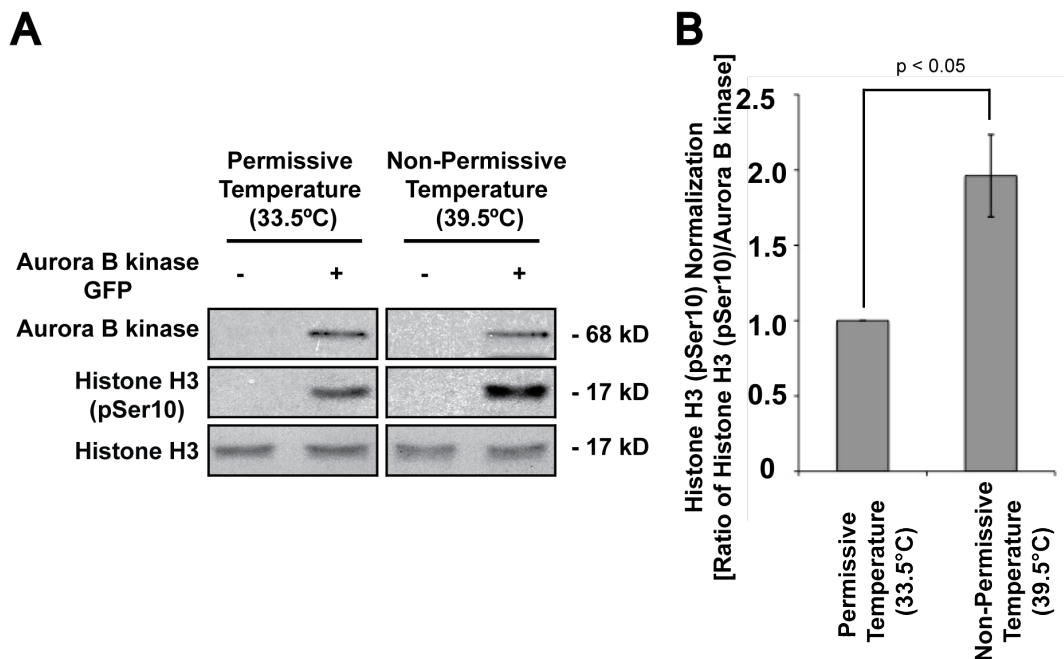


Figure 3.5.2: Diminished mitotic RanGTP enhances Aurora B kinase activity.

A) Kinase assay was conducted on Aurora B kinase protein immunoprecipitated from mitotic tsBN2 cells incubated at permissive or non-permissive temperature. Kinase activity was determined by phosphorylation of a known Aurora B kinase substrate, histone H3. Histone H3 was used as loading control. B) Quantified histone H3 (pSer10) intensities were normalized

and presented as relative fold change \pm s.d. (error bar) of three independent experiments. ($p < 0.05$, Student's t test).

3.6 Aurora B kinase inhibitor ZM447439 quells the chromosome misalignment phenotype

However, it was crucial to note that for the aforementioned postulation to be true, it was imperative to clarify whether the elevation in Aurora B kinase activity is consequence of the loss of tension at the kinetochores or vice versa. To address this, a known Aurora B kinase inhibitor, ZM447439, was used [76,77]. If the hyperactivity of Aurora B kinase preceeds the occurrence of aberrant chromosome displacement, inhibition of Aurora B kinase activity should circumvent the observed phenotype at non-permissive temperature. ZM447439 (500nM) was added with MG132 (10 μ M) for 2 hours prior to incubation at either permissive or non-permissive temperature (Fig. 3.6.1A). Preliminary checks via immunofluorescence and immunoblotting indicated that at a working concentration of 500nM, the inhibitor could efficiently inhibit the phosphorylation of Aurora B kinase at the kinetochores (Fig. 3.6.1B and C). Therefore this concentration of ZM447439 was used in the following experiments.

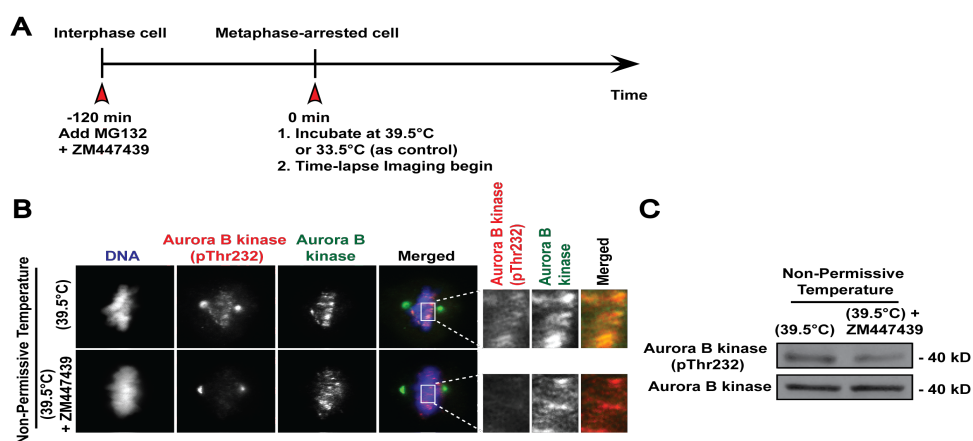


Figure 3.6.1: Phosphorylation of Aurora B kinase is sufficiently inhibited by Aurora B kinase inhibitor, ZM447439.

A) Schematic depiction of experimental conditions. ZM447439 was added with MG132 for 2 hours before incubation at permissive or non-permissive temperature. B) tsBN2 cells treated with or without ZM447439 were analyzed

by immunofluorescence staining with anti-Aurora B kinase and anti-Aurora B kinase (pThr232). Scale bar: 10 μ m. C) Western blot analysis of mitotic cells treated with ZM447439. Mitotic cells treated with the inhibitor exhibited decline in protein level of active Aurora B kinase. Actin was used as loading control.

Although gross chromosome misalignment was common for cells incubated at non-permissive temperature, it appeared that the severity of chromosome displacement was markedly reduced when the cells were treated with ZM447439. Only several errant miniscule chromosome clusters appeared to be displaced from the metaphase plate for cells treated with ZM447439 (Fig. 3.6.2, third panel) as compared to the temperature-shifted cells treated without the inhibitor (Fig. 3.6.2, middle panel).

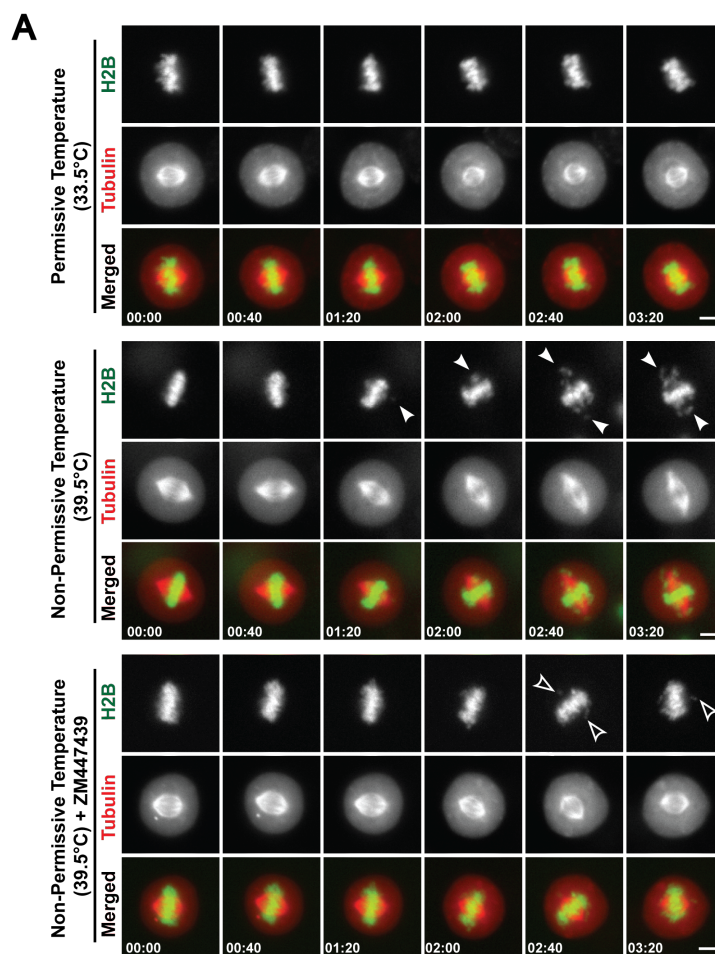


Figure 3.6.2: Aberrant Aurora B kinase activation compromises the fidelity of metaphase chromosome alignment.

Time-lapse imaging of tsBN2 cells expressing H2B-GFP and tubulin-mCherry. Control experiment at permissive temperature (upper panel), temperature-shift experiment (middle panel), temperature-shift + ZM447439 (Aurora B kinase inhibitor) experiment at non-permissive temperature (third panel). Chromosomes displaced from the metaphase plate are indicated by the arrowheads (Full arrowheads: grossly displaced chromosome clusters, empty arrowheads: miniscule chromosome clusters). Scale bar: 10 μ m.

Consistently, immunostaining analysis revealed that there were two populations of metaphase cells with a distinct difference in the severity of chromosome misalignment for metaphase cells incubated at non-permissive temperature (Fig. 3.6.3A). For quantification analysis, major misalignment was scored as large apparent chromosome clusters grossly displaced from the metaphase plate (Fig. 3.6.3A, middle panel) whereas minor misalignment describes metaphase cells with less than 3 minuscule 'lagging' chromosome clusters (Fig. 3.6.3A, third panel). Normal chromosomal alignment was denoted by tightly packed aggregation of chromosomes at the equator of the cell (Fig. 3.6.3A, first panel). Following that, quantification of more than 100 cells for each experimental set indicated that there was a significant reduction in the proportion of cells with major chromosome misalignment when temperature-shifted cells were treated with ZM447439 (Fig. 3.6.3B). Therefore, based on these results, it is likely that since active Aurora B kinase promotes the lability of kinetochore-microtubule attachment, aberrant activation of this kinase can compromise the stability of proper end-on attachments and thus lead to major chromosome misalignment in the absence of RanGTP.

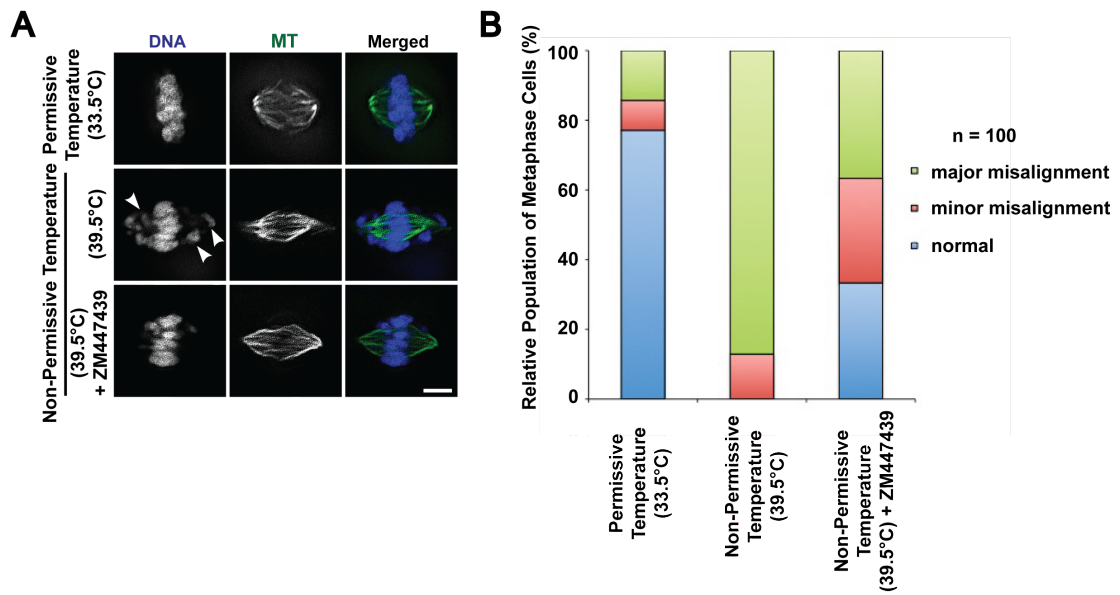


Figure 3.6.3: Regulated Aurora B kinase activation curbs the chromosome misalignment phenotype.

A) MG132-arrested tsBN2 cells were subjected to treatments as indicated. The cells were then fixed and stained with tubulin. Chromosomes displaced from the metaphase plate are indicated by the arrowheads. Scale bar: 10 μ m.

B) Quantified histogram illustrating proportion of metaphase cells with normal alignment, minor misalignment (<3 minuscule 'lagging' chromosome clusters) and major misalignment (>3 grossly displaced chromosomes clusters).

3.7 Kinetochore proteins; Hec1 and RanGAP1, spindle proteins; TPX2 and dynactin p150, and chromokinesin Kid are unperturbed by changes in RanGTP at metaphase

Localization of several kinetochore or motor proteins, which may be involved in the movement or maintenance of chromosome during mitosis were examined. Immunostaining results for Hec1, a component of the kinetochore KMN network, showed no difference in localization in metaphase cells incubated at either permissive or non-permissive temperature (Fig. 3.7.1A). Meanwhile, Ran regulator RanGAP1 that is found at the kinetochores during metaphase also maintained proper localization at the kinetochores for temperature-shifted metaphase cells (Fig. 3.7.1B). Likewise, for spindle-associated proteins, TPX2 and motor protein dynactin p150, localization of these proteins remained unchanged in both control and temperature-shifted cells (Fig. 3.7.1C and Fig. 3.7.1D). Therefore, exculpating their involvement in the manifestation of this observed phenotype.

Noting in mind that INCENP and Survivin are part of the chromosome passenger complex (CPC) along with Aurora B kinase, it was logical to consider the involvement of these CPC components. However, due to differences at the epitope recognition sites in human and hamster cells for these antibodies, it was not possible to further determine the involvement of these proteins through immunocytochemistry or immunoblotting. Similarly due to epitope differences in the hamster tsBN2 cells, I was unable to clarify the involvement of several core kinetochore and/or molecular motor proteins such as CENP-A, CENP-E, CENP-F and MCAK.

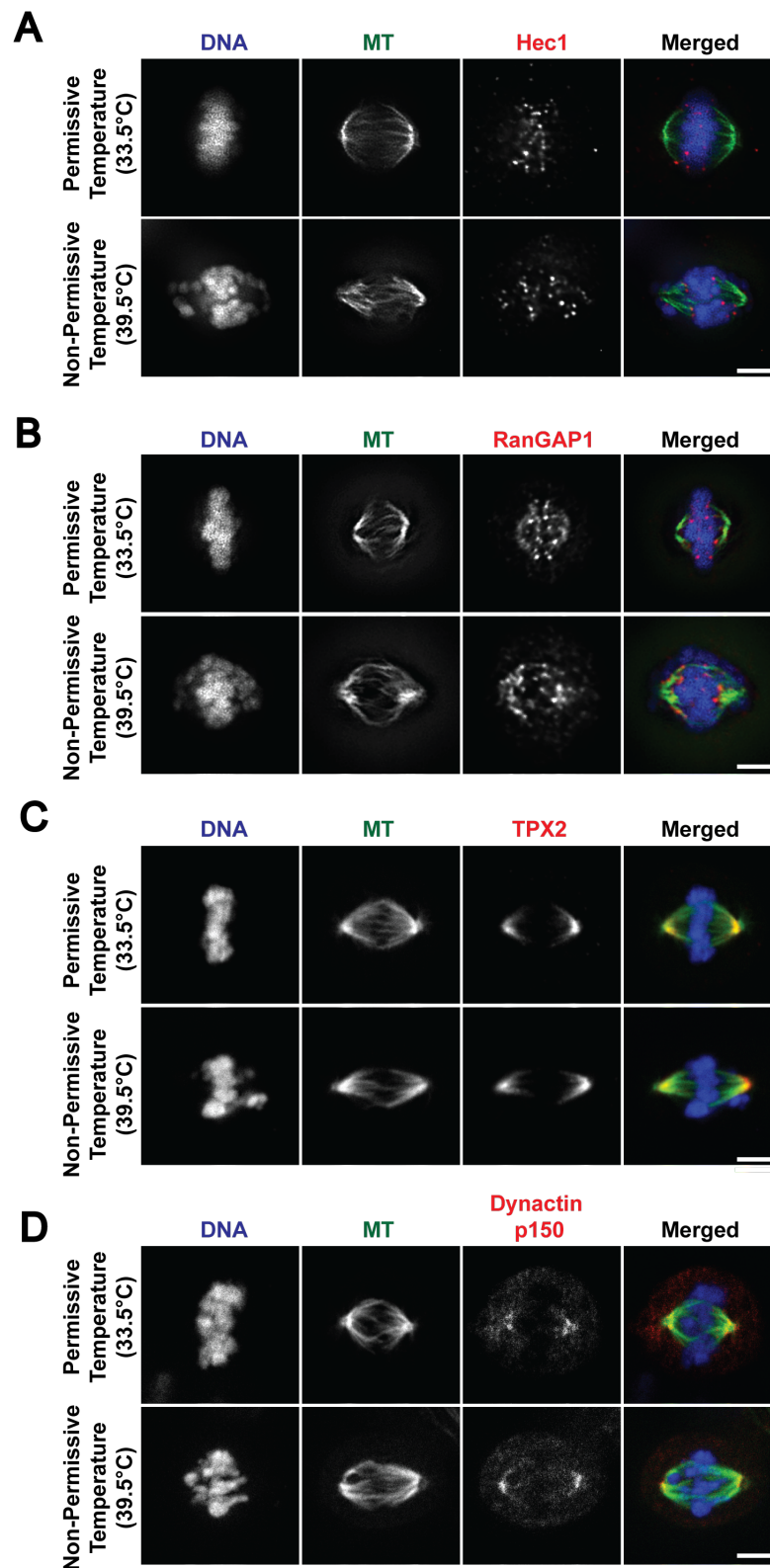


Figure 3.7.1: Localization of spindle protein TPX2, kinetochore proteins Hec1 and RanGAP1, and spindle motor dynactin-p150 are unaltered by RanGTP disruption.

Cells were immunostained with A) anti-Hec1 and tubulin B) anti-RanGAP1 and tubulin C) anti-TPX2 and tubulin D) anti-dynactin p150 and tubulin. Scale bar: 10 μ m.

Meanwhile, chromokinesin Kid, that had been previously reported to be involved in the maintenance of chromosome alignment at metaphase through depletion studies by injection of anti-Kid antibodies into metaphase-arrested *Xenopus* egg extracts, was also examined [25]. Although the Kid antibodies were unable to detect localization of the protein via immunocytochemistry, one of the antibodies was able to detect a specific band at approximately 73kDa. Immunoblotting results indicated that the protein level of Kid remained constant and was not degraded in temperature-shifted cells (Fig. 3.7.2). Hence, vindicating its involvement in the presentation of this observed RanGTP-deficient chromosome misalignment phenotype.

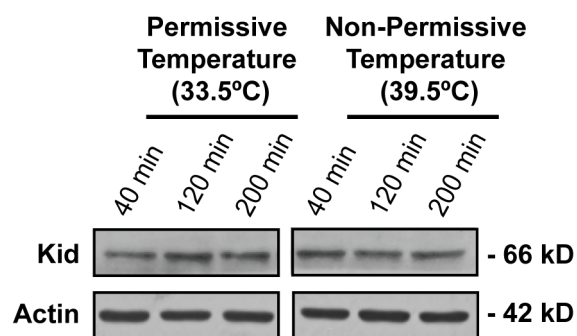


Figure 3.7.2: Chromokinesin Kid is not depleted after RanGTP depletion. Western blot analysis of mitotic tsBN2 cells incubated at permissive or non-permissive temperature and harvested via mechanical shake-off at various time points. Actin was used as loading control.

3.8 RanGTP-dependent Crm1 directs Mst1 to the kinetochores

During open mitosis in metazoans, in the absence of a nuclear membrane, components of the nucleocytoplasmic machinery can have significant roles to shuttle mitotic regulators such as SAFs for spindle assembly or Lamin B for spindle matrix reorganization respectively. One such example would be the nuclear export receptor Crm1. RanGTP-dependent Crm1 switches its role to a mitotic effector during mitosis by shuttling major mitotic regulators such as chromosome passenger proteins (CPCs) [30,32]. Under normal physiological conditions, Crm1 localizes to the kinetochores of metaphase cells. However, when mitotic cells were incubated at non-permissive temperature, Crm1 was significantly reduced at the kinetochores (Fig. 3.8.1A). Similarly, co-immunostaining with anti-tubulin shows a distinct loss of Crm1 at the kinetochore-microtubule attachment interface for temperature-shifted metaphase cells (Fig. 3.8.1B, lower panel).

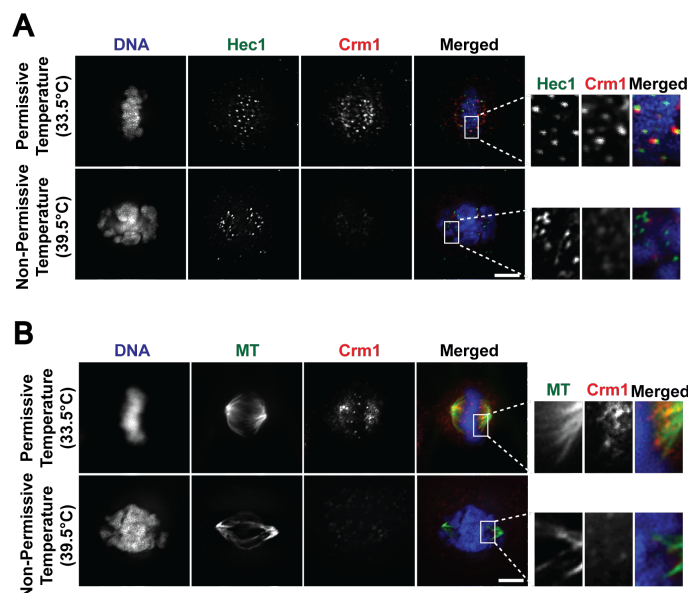


Figure 3.8.1: Mitotic effector Crm1 is significantly reduced from the kinetochores after RanGTP disruption.

Cells were immunostained with A) anti-Crm1 and anti-Hec1 B) anti-Crm1 and tubulin. Magnified images are shown on the right. Magnified merged image is exclusive of DNA. Scale bar: 10 μ m.

Meanwhile, NES-bearing Mst1 was recently reported to negatively regulate the mitotic activity of Aurora B kinase [52]. Notwithstanding the implications of this study, but more importantly, the aforementioned finding on Mst1 paved way for this study, especially since the mechanistic pathway and spatial coordination by which Mst1 exerts its inhibitory influence remains unknown. As Mst1 is an established Crm1 cargo, its involvement along the RanGTP-Crm1 axis in the manifestation of chromosome misalignment was speculated. At the permissive temperature, co-immunostaining of Crm1 and Mst1 showed colocalization at the spindle and at the kinetochores (Fig. 3.8.2A, upper panel). Similarly, upon increase of temperature to non-permissive temperature, the absence of Crm1 at the kinetochores also led to the loss of Mst1 at the kinetochores (Fig. 3.8.2A, lower panel). To verify whether there is any difference in the physical interaction between Crm1 and Mst1 after the increase in temperature, immunoprecipitation assay using anti-Mst1 antibody was conducted. Western blot analysis with anti-Crm1 or anti-Mst1 antibody indicated that whilst Crm1 and Mst1 protein levels remained similar for both temperatures in the input lanes, there was considerably reduced Crm1 protein immunoprecipitated in the temperature-shifted samples (Fig. 3.8.2B and C). These results indicate that the loss of RanGTP surrounding metaphase chromosomes led to the delocalization of Crm1 and the subsequent failure to recruit Mst1 to the kinetochores.

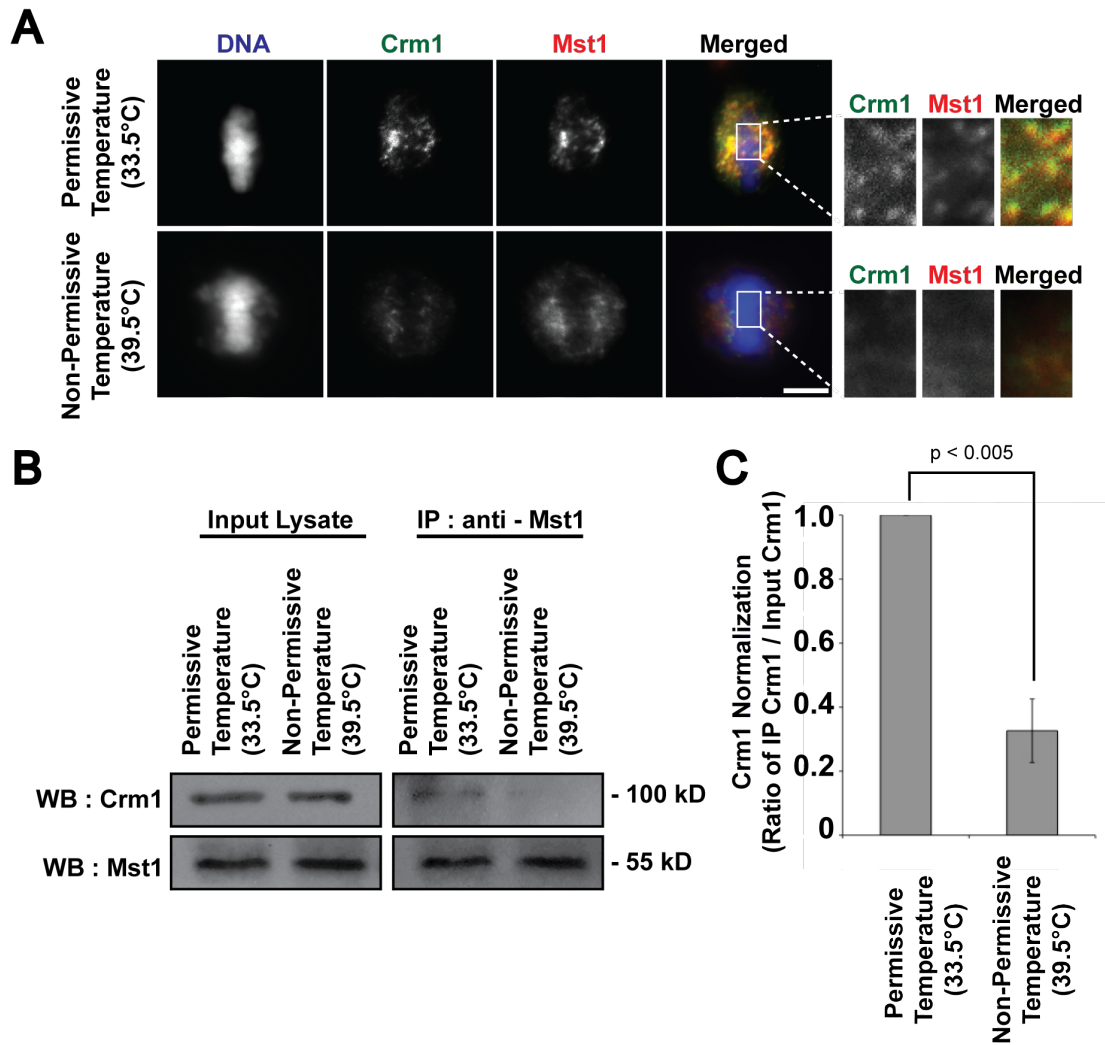


Figure 3.8.2: RanGTP-dependent Crm1 shuttles Mst1 to the kinetochores.

A) Cells were immunostained with anti-Crm1 and anti-Mst1 following incubation at permissive or non-permissive temperature. Magnified images are shown on the right. Magnified merged image is exclusive of DNA. Scale bar: 10 μ m. B) Immunoprecipitation assay was conducted using monoclonal anti-Mst1 antibody on mitotic cell lysates harvested 4 hours after incubation at permissive or non-permissive temperature. Immunoprecipitated proteins were analyzed by western blotting using antibodies against Crm1 and Mst1. C) Quantified Crm1 intensities were normalized and presented as relative fold change \pm s.d. (error bar) of three independent experiments. ($p < 0.005$, Student's t test).

3.9 Functional Mst1 at the kinetochores maintains stable kinetochore-microtubule attachments

In order to investigate the contribution of Mst1 in relation to RanGTP levels, rescue experiments were conducted by overexpressing Mst1 wild-type or Mst1 kinase dead K59R mutant in tsBN2 cells and subsequently incubating the mitotic cells at non-permissive temperature. Time-lapse images showed that cells with Mst1 WT-mCherry overexpression reinstated properly aligned metaphase chromosomes even at non-permissive temperature (Fig. 3.9.1A, top panel). However, metaphase cells with kinase-dead mutant, Mst1 K59R-mCherry transfection exhibited chromosome misalignment when RanGTP was abrogated (Fig. 3.9.1A, middle panel). Similarly, cells transfected with the mCherry plasmid as a control exhibited aberrant chromosome alignment when incubated at non-permissive temperature (Fig. 3.9.1A, third panel). This indicated that functionally intact Mst1 is necessary for the maintenance of stable kinetochore-microtubule attachments and thus ensures proper chromosome alignment during metaphase. Bearing in mind that Mst1 exerts its influence on Aurora B kinase at the kinetochores, the abundant overexpression of Mst1 WT or K59R-mCherry fusion protein was detected throughout the cell and this would enable the non-native proteins to outcompete and exert their influence on Aurora B kinase at the kinetochores. Correspondingly, immunoblotting of protein levels of Mst1 confirm that the levels of non-native Mst1 is significantly higher in expression as compared to the endogenous Mst1 protein levels (Fig. 3.9.1B).

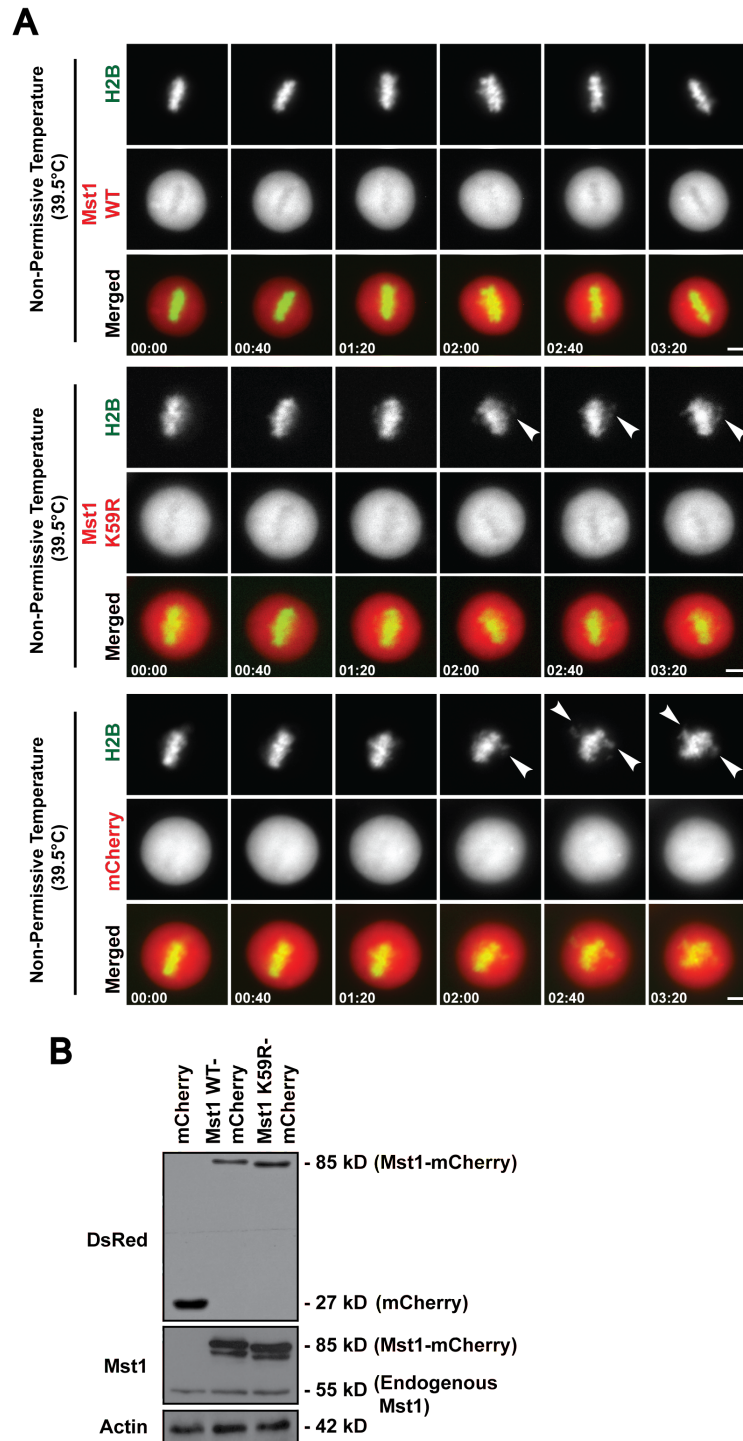


Figure 3.9.1: Overabundant of wild-type Mst1 restores the stability of kinechore-microtubule attachment for proper metaphase chromosome alignment.

A) Time-lapse imaging of tsBN2 cells expressing H2B-GFP and Mst1 WT-mCherry, Mst1 K59R-mCherry or mCherry (positive control). Overexpression of Mst1 WT abrogated the misalignment phenotype in cells incubated at non-permissive temperature. Chromosomes displaced from the metaphase plate are indicated by the arrowheads. Scale bar: 10 μ m. B) Western blot analysis of mitotic cell lysates indicating levels of endogenous and non-native Mst1 protein. Actin was used as loading control.

If Mst1 functions as an effector of RanGTP in maintaining the stability of kinetochore-microtubule attachments, then the loss of Mst1 irrespective of RanGTP's existence can render metaphase chromosomes susceptible to misalignment. Hence, to further verify Mst1's role in regulating the stability of kinetochore-microtubule attachments, Mst1 was depleted by RNA interference. Endogenous Mst1 knockdown efficiency of 70-80% was achieved in tsBN2 cells (Fig. 3.9.2A and B). Further qualitative inspection also indicated a significant depletion of Mst1 (Fig. 3.9.2C) in these cells. In corroboration with the aforementioned postulation, quantification of metaphase cells silenced with control or Mst1 siRNA showed that when Mst1 was depleted there was an appearance of a significant proportion of metaphase cells with chromosome misalignment (Fig. 3.9.2D).

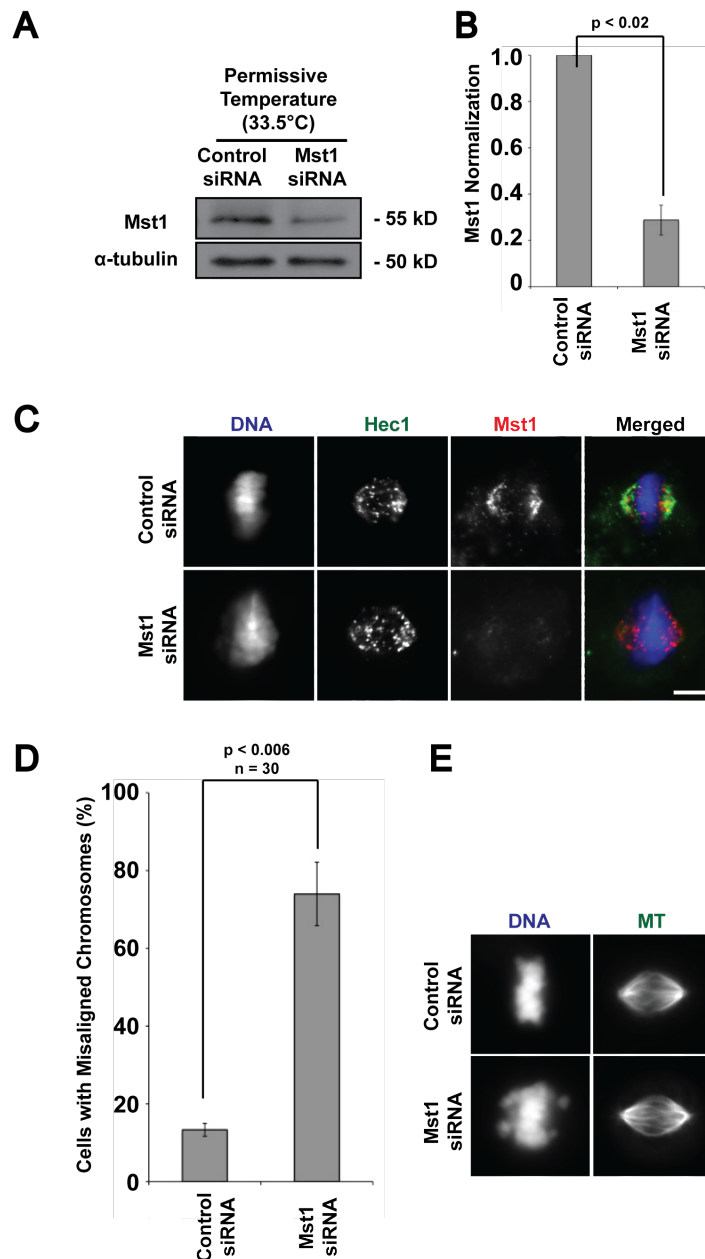


Figure 3.9.2: Mst1 is indispensable to maintain proper chromosome alignment at metaphase.

Knockdown of Mst1 by RNAi in tsBN2 cells. A) Western blot analysis of mitotic cells transfected with control or Mst1 siRNA. Tubulin was used as loading control. B) Quantified Mst1 intensities were normalized and presented as relative fold change \pm s.d. (error bar) of three independent experiments. ($p < 0.02$, Student's t test). C) Cells were immunostained with anti-Mst1 and anti-Hec1. Metaphase cells depleted of Mst1 shows loss of Mst1 localization at the kinetochores. ($n = 30$) D) Histogram shows percentage of fixed cells with misaligned chromosomes. Error bars show \pm s.d. from three independent experiments. ($p < 0.006$, Student's t test). E) Representative images of the majority population of metaphase cells incubated with control or Mst1 RNAi. Scale bar: 10 μ m.

Similarly when Mst1 expression is silenced in HeLa cells, an increase in the proportion of metaphase cells with misaligned chromosomes was detected (Fig. 3.9.3A). Although the amount of RNAi used was similar to that for tsBN2 cells, knockdown efficiency in HeLa cells was only approximately 50% (Fig. 3.9.3C and D). Even so, a significant population of metaphase cells still exhibited aberrantly aligned metaphase chromosomes. Therefore, these results presented prove that Mst1 is indeed a functionally indispensable effector of RanGTP in maintaining the fidelity of chromosome alignment during metaphase.

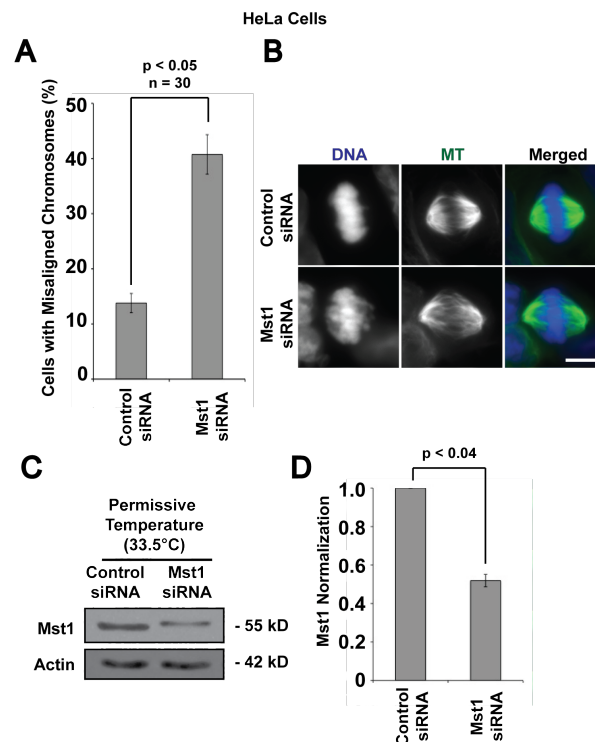


Figure 3.9.3: Mst1 depletion compromises stable metaphase chromosome alignment in HeLa cells.

Knockdown of Mst1 by RNAi in HeLa cells. A) Histogram shows percentage of fixed cells with misaligned chromosomes. Error bars show \pm s.d. from three independent experiments. ($p < 0.05$, Student's *t* test). B) Representative images of the majority population of metaphase cells incubated with control or Mst1 RNAi. Scale bar: 10 μ m. C) Western blot analysis of mitotic cells transfected with control or Mst1 siRNA. Actin was used as loading control. D) Quantified Mst1 intensities were normalized and presented as relative fold change \pm s.d. (error bar) of three independent experiments. ($p < 0.04$, Student's *t* test).

3.10 RanGTP-dependent Mst1 binds to and represses active Aurora B kinase activity

Next, immunoprecipitation assay was conducted to ascertain whether Aurora B kinase interacts with Mst1 and that Mst1 exerts its inhibitory influence directly on Aurora B kinase at the kinetochores. Preliminary Immunoprecipitation assay conducted using endogenously expressed Aurora B kinase and Mst1 showed that Aurora B kinase was immunoprecipitated with Mst1 at permissive temperature. However, there was significantly reduced Aurora B kinase from the samples incubated at non-permissive temperature (Fig. 3.10.1A and B). This suggests that Aurora B kinase may be a substrate of Mst1 whose activity is affected by the loss of RanGTP. To further examine the nature of the interaction between Mst1 and Aurora B kinase, Aurora B kinase and Mst1 were overexpressed in HEK cells using Aurora B kinase-GFP and FLAG-tagged Mst1 wild-type (WT), K59R or K59R Δ C (amino acid 1-330, lacking NES, and kinase activity) plasmids respectively. Although immunoprecipitation results showed minor decline in Mst1-K59R and Aurora B kinase interaction (Fig. 3.10.1C), a more significant observation was that the NES-deficient mutant (K59R Δ C) showed distinct reduction in Aurora B kinase binding (Fig. 3.10.1 E and F). This result here suggests that the interaction between Mst1 and Aurora B kinase is NES-dependent.

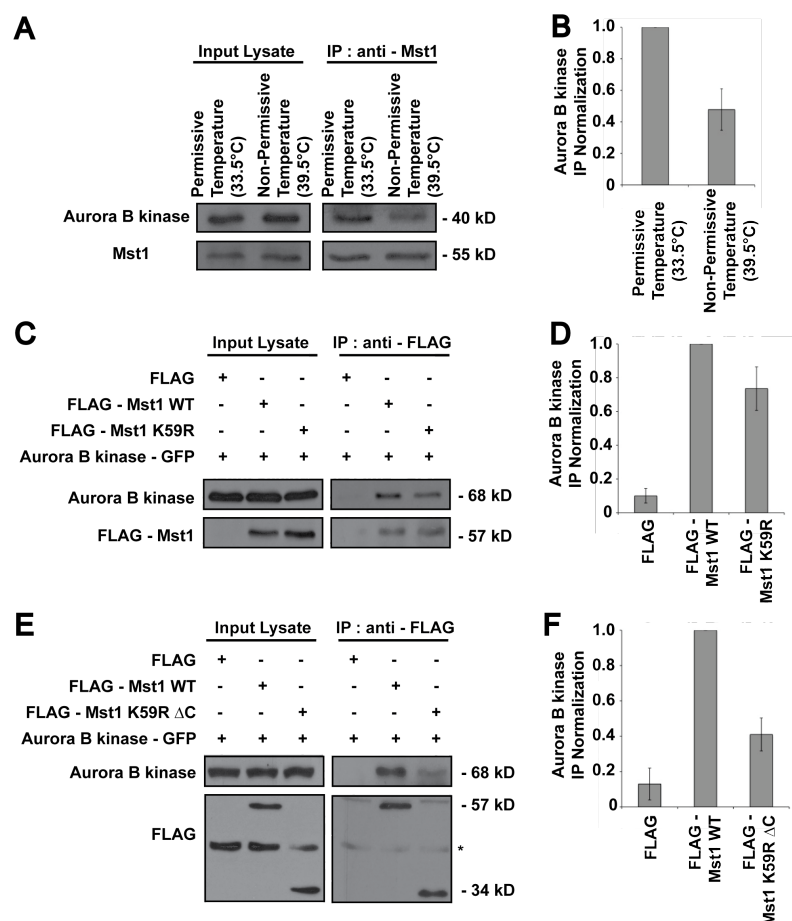


Figure 3.10.1: Robust interaction of functionally active Mst1 with Aurora B kinase.

A) Immunoprecipitation assay was conducted using anti-Mst1 antibody on mitotic tsBN2 cell lysates harvested 4 hours after incubation at permissive or non-permissive temperature. B) Quantified Aurora B kinase intensities were normalized and presented as relative fold change \pm s.d. (error bar) of three independent experiments. ($p < 0.02$, Student's t test). C) Immunoprecipitation assay was conducted using monoclonal anti-FLAG antibody on metaphase-enriched HEK cell lysates co-transfected with FLAG, FLAG-Mst1 WT or FLAG-Mst1 K59R and Aurora B kinase-GFP. Immunoprecipitated proteins were analyzed by western blotting using antibodies against Aurora B kinase and FLAG. D) Quantified Aurora B kinase intensities were normalized against immunoprecipitated Aurora B kinase co-transfected with FLAG-Mst1 WT and presented as relative fold change \pm s.d. (error bar) of three independent experiments. ($p < 0.001$, One way ANOVA). E) Immunoprecipitation assay was conducted using monoclonal anti-FLAG antibody on metaphase-enriched HEK cell lysates co-transfected with FLAG, FLAG-Mst1 WT or FLAG-Mst1 K59R Δ C and Aurora B kinase-GFP. Immunoprecipitated proteins were analyzed by western blotting using antibodies against Aurora B kinase and FLAG. F) Quantified Aurora B kinase intensities were normalized against immunoprecipitated Aurora B kinase co-transfected with FLAG-Mst1 WT and presented as relative fold change \pm s.d. (error bar) of three independent experiments. ($p < 0.001$, One way ANOVA). Asterisk (*) indicates non-specific bands.

A further examination on the levels of active Aurora B kinase confirmed that wild-type Mst1 does negatively regulate the autophosphorylation of Aurora B kinase. Levels of active Aurora B kinase appeared suppressed in the presence of overexpressed FLAG-Mst1 WT but remained high for samples with control FLAG plasmid, FLAG-Mst1 mutant plasmid transfections (Fig. 3.10.2). Therefore results reaffirm that Aurora B kinase is indeed a downstream substrate of Mst1 in this RanGTP-dependent maintenance of metaphase chromosome alignment.

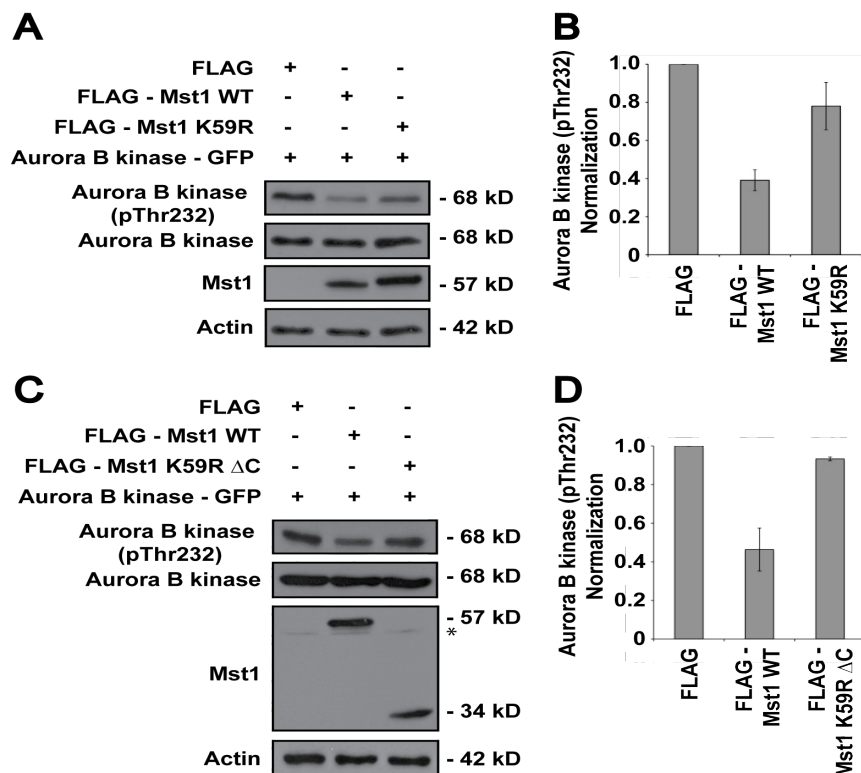


Figure 3.10.2: Wild-type Mst1 represses active Aurora B kinase activity.

A) Western blot analysis of metaphase-enriched HEK cells co-transfected with Aurora B kinase and FLAG, FLAG-Mst1 WT or FLAG-Mst1 K59R. B) Quantified active Aurora B kinase intensities were normalized and presented as relative fold change \pm s.d. (error bar) of three independent experiments. ($p < 0.05$, One way ANOVA). C) Western blot analysis of metaphase-enriched HEK cells co-transfected with Aurora B kinase and FLAG, FLAG-Mst1 WT or FLAG-Mst1 K59R Δ C. B) Quantified active Aurora B kinase intensities were normalized and presented as relative fold change \pm s.d. (error bar) of three independent experiments. ($p < 0.05$, One way ANOVA). Asterisk (*) indicates endogenous Mst1. Actin was used as loading control.

In addition, further immunofluorescence analysis on metaphase chromosome spreads of cells overexpressing Mst1-mCherry fusion proteins showed that intact NES is important for the shuttling of Mst1 within the vicinity of the chromosome including the kinetochore for interaction with Aurora B kinase. As expected, Mst1 WT-mCherry fusion protein can be detected at the kinetochores (Fig. 3.10.3C, upper panel). However, a distinct absence was observed for Mst1 K59R Δ C (Fig. 3.10.3C, lower panel). These results thus indicate that the presence of the NES on Mst1 is thus important for its recruitment to the kinetochores by Crm1 for robust interaction between Mst1 and Aurora B kinase and to allow for Mst1 to directly limit the activity of Aurora B kinase. Hence, it can be concluded that functionally intact Mst1 is necessary to regulate the activity of Aurora B kinase in the preservation of stable kinetochore-microtubule attachments and thus proper chromosome alignment at metaphase.

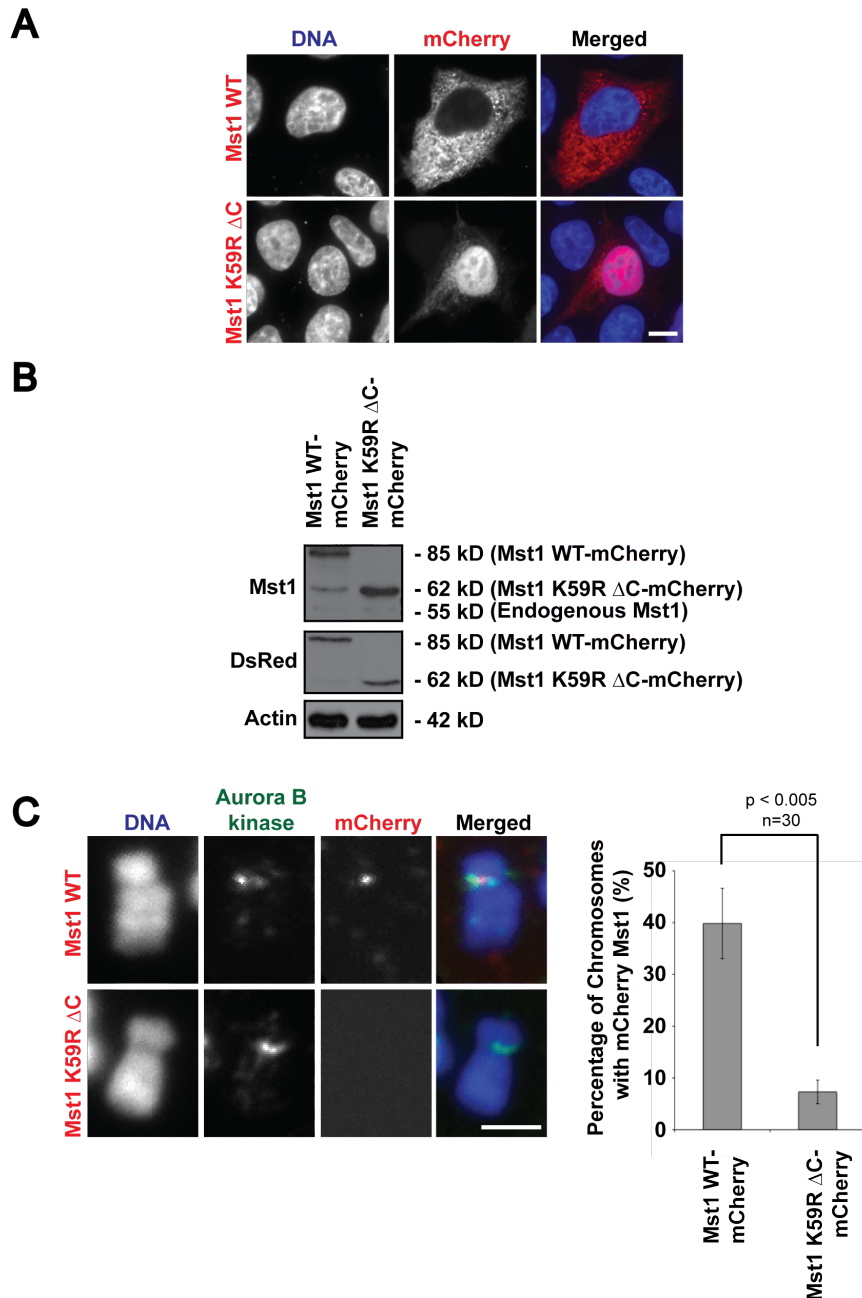


Figure 3.10.3: Functionally intact Mst1 is recruited to kinetochores of metaphase chromosomes.

A) Interphase cells expressing Mst1-WT or K59R Δ C-mCherry were fixed and subjected to immunofluorescence analysis. Mst1 K59R Δ C mutant lacking NES shows distinct accumulation in the nucleus. Scale bar: 10 μ m. B) Western blot analysis of Mst1 and mCherry (DsRed) from mitotic tsBN2 cells transfected with control mCherry, Mst1 WT-mCherry or Mst1 K59R Δ C-mCherry showing multifold increase in levels of Mst1 in cells transfected with Mst1-mCherry. Actin was used as loading control. C) Metaphase spread of tsBN2 cells expressing Mst1 WT or K59R Δ C-mCherry were immunostained with anti-Aurora B kinase. Scale bar: 2 μ m. D) Histogram shows percentage of metaphase chromosomes with Mst1-mCherry fusion protein. Error bars show \pm s.d. from three independent experiments. ($p < 0.005$, Student's t test).

Chapter 4 : Discussion

4.1 *In vivo* FRET imaging revealed novel regulatory role of RanGTP at metaphase

With the use of the Rango biosensor and FRET based on the Correction-Youvan Method, an approach that allows visualization of changes in RanGTP levels in parallel with phenotypic changes of chromosomes upon temperature change in tsBN2 cells was developed. Although Rango and FRET have been previously used to study Ran, it has not been applied to simultaneously visualize changes in RanGTP and its resulting cellular perturbations. With this approach, real-time changes in chromosome orientation observed after increase in temperature could be correlated to the corresponding changes in RanGTP distribution at a single cell level.

Under sustained MG132 treatment, metaphase cells with robust RanGTP levels should have already achieved proper, end-on amphitelic kinetochore-microtubule attachments for stable alignment of chromosomes at the metaphase plate, as indicated by control metaphase cells incubated at permissive temperature. Interestingly, FRET time-lapse imaging results revealed that upon increase in temperature to non-permissive temperature, the decay in RanGTP concentration led to a progressive misalignment of metaphase chromosomes displaced from the equator. Whilst the misaligned chromosomes may appear to exhibit prometaphase-like chromosome morphology observed when chromosomes are congressing, with chromosome distribution along the spindle microtubules and at the metaphase plate, the *in vivo* FRET time-lapse imaging method applied here provided proof that the directionality of aberrantly aligned chromosomes are

opposite that of congressing chromosomes and thus reveal a novel event at metaphase which is regulated by the mitotic RanGTP.

4.2 Hyperactivated Aurora B kinase acts as an instigator to promote promiscuous kinetochore-microtubule attachments

With the mitotic spindle intact, aberrantly aligned chromosomes were characterized as either having lost proper amphitelic attachment or loss of attachment to spindle microtubules altogether (Fig. 3.4.2A and B). Under normal circumstances, tension imbalance across the kinetochores would be detected by Aurora B kinase and a signal generated for SAC activation [49,78]. In agreement, there was a prominent increase in Aurora B kinase activity (Fig. 3.5.1A-D and Fig. 3.5.2A-B) and reactivation of the SAC with the recruitment of BubR1 in RanGTP-depleted cells (Fig. 3.4.3A and B). Given that active Aurora B kinase can readily modulate kinetochore-microtubule dynamics, it was of interest to speculate on its involvement in the presentation of the observed chromosome misalignment phenotype. However, when a known Aurora B kinase inhibitor, ZM447439, was used to treat metaphase cells incubated at non-permissive temperature, it was surprising to observe a prominent re-emergence of the proportion of metaphase cells with normal alignment and an appearance of a population with minor misalignment of chromosomes. This was of an improvement to temperature-shifted metaphase cells without any inhibitor treatment (Fig. 3.6.3A and B). The use of the Aurora B kinase inhibitor appeared to dampen the severity of the aberrantly aligned chromosomes displaced from the equator. To date, Aurora B kinase's role at the kinetochore is established as a protagonist to rectify erroneous kinetochore-microtubule attachments rather than as the instigator to aberrant attachment and chromosome orientation [77,79]. Therefore, the decline in the population of cells with major chromosome misalignment was

unexpected. However, it is important to note that whilst the pre-established tension sensor and error correction role is indispensable at the initial chromosome congression stage during the search and capture process for kinetochore-microtubule attachments to form and stabilize, it is likely that after formation of stable metaphase chromosome alignment, the role of Aurora B kinase in correcting erroneous attachment becomes less prominent as its role shifts towards regulating the SAC signaling and anaphase onset [80,81]. In the context of this study, proper chromosome alignment has already formed prior to RanGTP depletion and subsequent appearance of chromosomes displaced from the equator. Therefore it is likely that at this transitional stage between chromosome congression and segregation, the unrestricted hyperphosphorylation of Aurora B kinase due to the loss of RanGTP at metaphase inadvertently causes Aurora B kinase to promote promiscuous kinetochore-microtubule reorientation, resulting in the observed chromosome misalignment phenotype. By showing that the chromosome misalignment phenotype at non-permissive temperature is curbed when Aurora B kinase activity is suppressed with the use of ZM447439, and with Mst1 overexpression (Fig. 3.10.2, to be discussed later), it is likely that Aurora B kinase's role at the kinetochore is negatively altered in the absence of RanGTP. Therefore, the data presented here does implicate Aurora B kinase in the manifestation of the chromosome misalignment phenotype when RanGTP is depleted.

4.3 Formation of RanGTP-Crm1-Mst1 ternary complex dictates the state of metaphase chromosome alignment

In dissecting the role of RanGTP in the observed phenotype, it was logical to review its involvement from the perspective of its conserved transport and processes. Even in mitosis, RanGTP acts in concert with key transport components such as the importins and is dependent on its regulators: RCC1, RanGAP1 and RanBP [82,83]. In concurrence, during mitosis, RanGTP-associated nuclear transport receptor Crm1 and Ran regulator RanGAP1 are localized to the kinetochores [32]. A robust concentration of mitotic RanGTP is thus rudimentary for Crm1 cargo loading since its role hinges on the formation of the RanGTP, Crm1, and NES-bearing cargo ternary complex. In addition, the positioning of RanGAP1 at the kinetochores allows for liberation of shuttled cargoes near the kinetochores. In the context of this study, hypothetically there should be a cargo that harbors a functional NES and is positioned upstream of Aurora B kinase's signaling pathway and/or is involved in Aurora B kinase's regulatory feedback mechanism. In view of this, Mst1 was shortlisted as a potential candidate.

Although Mst1 is an established NES-bearing cargo in the RanGTP-dependent nuclear transport pathway, much of the existing knowledge on this kinase has been concentrated on its involvement in response to cellular stress and apoptotic stimuli as well as in a apoptosis-related lineage specific cellular programming [56,58,84]. Interestingly, this kinase was recently shown to have a novel and non-apoptotic regulatory function in mitosis. Notably and in concordance with my hypothesis, Mst1 was reported to negatively regulate Aurora B kinase activity via the modulation of the autophosphorylation state of

active Aurora B kinase [52]. Data presented here confirmed that in the presence of abundant RanGTP during metaphase, Crm1 recruits the NES-bearing Mst1 to the kinetochores (Fig. 3.8.2A). In addition, quantified intensities of immunoprecipitated Crm1 indicated a substantial reduction in Crm1-Mst1 interaction when RanGTP is depleted (Fig. 3.8.2C).

Notwithstanding the significance of but rather in concordance with my results, aberrantly aligned chromosomes were detected when leptomycin B was used to inhibit Crm1 [32]. Moreover, in cells depleted of Mst1, misaligned metaphase chromosomes were observed (Fig. 3.9.2D and E). Taken together, these implied that a ternary complex formation, along the order of RanGTP-Crm1-Mst1, is rudimentary in regulating the stability of kinetochore-microtubule attachments at metaphase, after proper chromosome congression.

Moreover, immunoprecipitation assay conducted indicated that endogenous Aurora B kinase binds to Mst1 robustly and this interaction is compromised in cells incubated at non-permissive temperature wherein RanGTP is depleted (Fig. 3.10.1A-B). In attempts to determine the nature of the interaction between these two proteins, Aurora B kinase-GFP and FLAG-Mst1 WT or Mst1 mutants were co-transfected and overexpressed, Although a minor compromise in interaction was observed with the kinase-dead form of Mst1, Mst1 K59R, there was no substantial reasoning to account for the decline in binding (Fig. 3.10.1C and D). Nonetheless, a more significant finding was observed with the distinct reduction in efficiency of Mst1-Aurora B kinase interaction when the NES-deficient mutant, Mst1 K59R Δ C, was overexpressed instead (Fig. 3.10.1E and F). In agreement, immunostaining of

metaphase chromosomes overexpressing Mst1 WT or K59R Δ C-mCherry fusion protein also showed that the NES-deficient mutant failed to localize to the kinetochore with Aurora B kinase (Fig. 3.10.3C). These data reveal the importance of the NES on Mst1 for interaction with Aurora B kinase and also in the earlier mentioned recruitment of Mst1 along the proposed hypothesis of the RanGTP-Crm1-Mst1 ternary complex formation to shuttle Mst1 to the kinetochores for interaction with and to curtail Aurora B kinase's influence on kinetochore-microtubule dynamics.

4.4 RanGTP-dependent regulation of Aurora B kinase determines its influence on kinetochore-microtubule attachments

Although earlier studies have affirmed RanGTP's role in mitotic spindle formation and chromosome segregation [23,85,86], the involvement of RanGTP in maintenance of chromosome alignment at metaphase has yet to be established. The results presented here describe a new role for the mitotic RanGTP that bridges the molecular chronological gap between chromosome congression and chromosome segregation. The depletion of RanGTP during metaphase leads to the failure of Crm1 in recruiting Mst1 to the kinetochore (Fig. 3.8.2A-C). As consequence, autophosphorylation of Aurora B kinase and thus its basal kinase activity is escalated (Fig. 3.5.1A-D and Fig. 3.5.2A-B). Results presented here provide proof that in the absence of RanGTP, deregulation of Aurora B kinase's phosphorylation state can inadvertently tip the balance of its role from a protagonist to an antagonist in modulating kinetochore-microtubule attachments. The unrestricted hyperphosphorylation of Aurora B kinase intensifies its activity towards promoting the destabilization

of kinetochore-microtubule attachments and stimulation of promiscuous reorientation of kinetochore-microtubule attachments (Fig. 4.4). Not surprisingly, the upregulation of Aurora B kinase activity has been associated with genomic instability and oncogenic transformations in human cells. Considering Aurora B kinase's role in establishing proper kinetochore-microtubule attachments and ensuring equal partitioning of genetic materials into daughter cells, precise regulation of Aurora B kinase activity is essential to prevent formation of aneuploid or euploid cells which culminates towards tumorigenesis [50,87].

In summary, this study here has shown that the presence of high mitotic RanGTP is indeed critical for the maintenance of kinetochore-microtubule attachments at metaphase. Data presented has revealed RanGTP as the unifying positioning system that links the spatial regulation of Mst1-Aurora B kinase interaction to keep Aurora B kinase's activity in check and thus ensuring the stability of kinetochore-microtubule attachments. By promoting stable chromosome alignment and thus allowing equal chromosome segregation, this regulatory role of RanGTP governs the precise process of chromosome partitioning. Thus, RanGTP is key in protecting the fidelity of mitotic progression to maintain genomic integrity and for prevention of tumorigenesis.

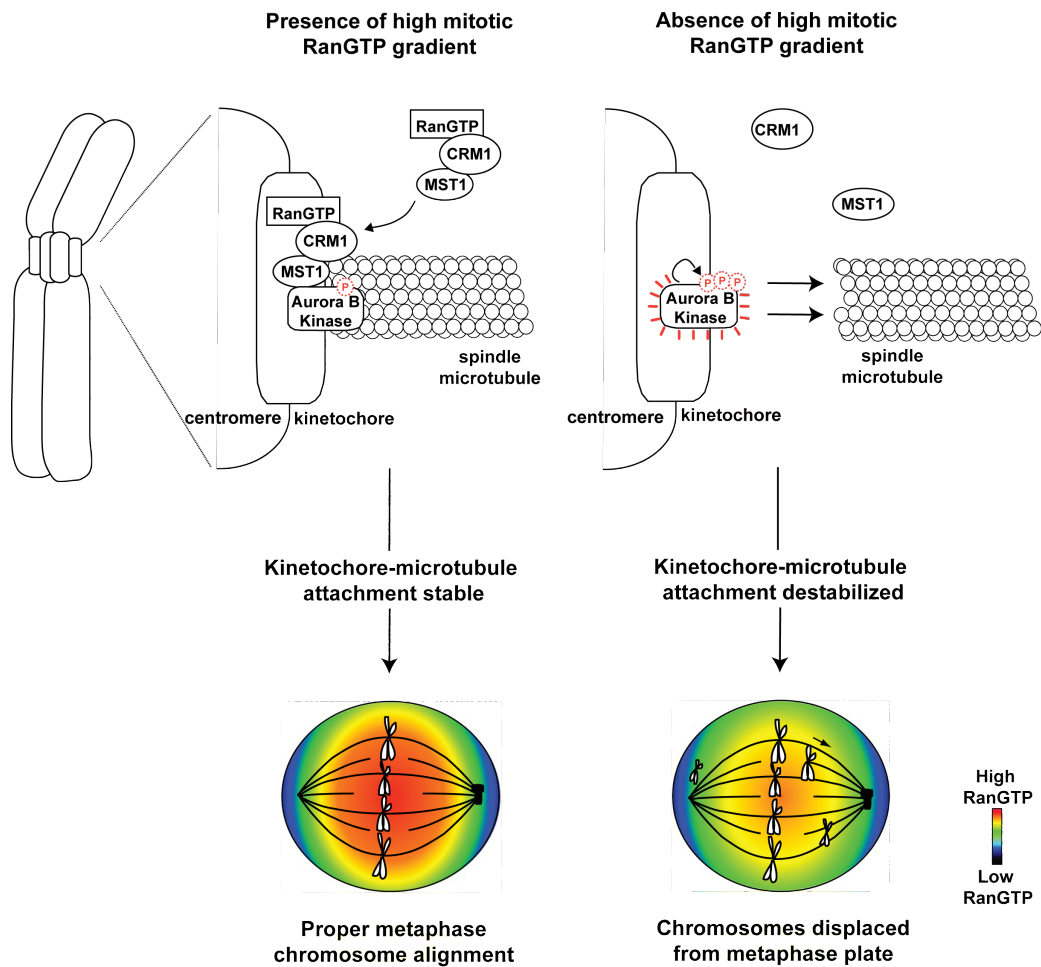


Figure 4.4: Model illustrating the role of mitotic RanGTP in preserving stable chromosomal alignment during metaphase.

In the presence of high mitotic RanGTP, Crm1 localizes to the kinetochore. Mst1 is then recruited as part of the RanGTP-Crm1-Mst1 ternary complex. Presence of Mst1 limits the autophosphorylation of Aurora B kinase and thus stabilizes kinetochore-microtubule attachments. This results in stable chromosome alignment at the metaphase plate (Left panel). When RanGTP depleted, Crm1 is unable to bind to and target Mst1 to the kinetochore. Consequently, Aurora B kinase becomes hyperactivated to promote kinetochore-microtubule reorientation. The loss of proper amphitelic attachment ensues leading to the displacement of metaphase chromosomes from the equator (Right panel).

4.5 RanGTP In Anti-cancer Therapies

Judging from RanGTP's wide-ranging roles in regulating the plethora of processes in mitosis, precise regulation and proper functional Ran machinery is indispensable. Dysregulation of the Ran system can lead to errors in mitosis, which, if left unchecked, give rise to aneuploid daughter cells, which predisposes cancerous transformations. Whilst it may seem tempting to speculate on RanGTP's potential to be translated to the development of novel therapies to curb tumor progression, manipulation of this protein should be executed with care, especially since it is implicated in the regulation of multiple intricate processes in mitosis. Hence, there has been an emphasis in acquiring a comprehensive body of knowledge on the mechanistic actions of RanGTP, prior to applying it as a therapeutic option. Therefore, it is not surprising that existing anti-cancer therapeutics based on RanGTP are primarily focused on the molecular targets of RanGTP, such as Plk1, Aurora A kinase and Eg5 [88,89,90].

Even so, the prospects of RanGTP in anti-cancer therapies should not be undermined. With unwaning interest in and a growing knowledge on this protein, the suitability of RanGTP in cancer therapies is further affirmed. This is especially since deficiency in mitotic RanGTP has been shown to result in defective mitotic spindles and chromosome missegregations that are associated with prolonged mitotic checkpoint arrest which can culminate in mitotic cell death, especially in tumor cells [91,92]. Importantly, this absence of RanGTP is well adapted by many normal cells without mitotic defects [92]. As such, there has been considerable interest in utilizing Ran-binding proteins

to manipulate RanGTP levels in cells to simulate pro-apoptotic environments especially in cancerous cells [93,94]. Additionally, a recent study has shown considerable success in eliminating highly proliferative cancer cells in a combinatorial treatment of Ran silencing and anti-cancer drug Gefinitib [36]. Considering that the application of RanGTP in anti-cancer therapies is still at best, at its infancy stage, there are unlimited avenues to explore and to further tap on RanGTP's potential as an effective cancer treatment.

REFERENCES

1. Lee JY, Orr-Weaver TL (2001) The molecular basis of sister-chromatid cohesion. *Annual review of cell and developmental biology* 17: 753-777.
2. Zarzov P, Decottignies A, Baldacci G, Nurse P (2002) G(1)/S CDK is inhibited to restrain mitotic onset when DNA replication is blocked in fission yeast. *The EMBO journal* 21: 3370-3376.
3. Zhang D, Nicklas RB (1996) 'Anaphase' and cytokinesis in the absence of chromosomes. *Nature* 382: 466-468.
4. Li X, Nicklas RB (1995) Mitotic forces control a cell-cycle checkpoint. *Nature* 373: 630-632.
5. Zhou J, Yao J, Joshi HC (2002) Attachment and tension in the spindle assembly checkpoint. *Journal of cell science* 115: 3547-3555.
6. Doncic A, Ben-Jacob E, Einav S, Barkai N (2009) Reverse engineering of the spindle assembly checkpoint. *PloS one* 4: e6495.
7. Matsuoka S, Ballif BA, Smogorzewska A, McDonald ER, 3rd, Hurov KE, et al. (2007) ATM and ATR substrate analysis reveals extensive protein networks responsive to DNA damage. *Science* 316: 1160-1166.
8. Lukas J, Lukas C, Bartek J (2004) Mammalian cell cycle checkpoints: signalling pathways and their organization in space and time. *DNA repair* 3: 997-1007.
9. Dai W, Wang Q, Liu T, Swamy M, Fang Y, et al. (2004) Slippage of mitotic arrest and enhanced tumor development in mice with BubR1 haploinsufficiency. *Cancer research* 64: 440-445.
10. Schliekelman M, Cowley DO, O'Quinn R, Oliver TG, Lu L, et al. (2009) Impaired Bub1 function in vivo compromises tension-dependent checkpoint function leading to aneuploidy and tumorigenesis. *Cancer research* 69: 45-54.
11. Michel LS, Liberal V, Chatterjee A, Kirchwegger R, Pasche B, et al. (2001) MAD2 haplo-insufficiency causes premature anaphase and chromosome instability in mammalian cells. *Nature* 409: 355-359.
12. Moore W, Zhang C, Clarke PR (2002) Targeting of RCC1 to chromosomes is required for proper mitotic spindle assembly in human cells. *Current biology : CB* 12: 1442-1447.
13. Ciciarello M, Mangiacasale R, Lavia P (2007) Spatial control of mitosis by the GTPase Ran. *Cell Mol Life Sci* 64: 1891-1914.
14. Clarke PR, Zhang C (2008) Spatial and temporal coordination of mitosis by Ran GTPase. *Nat Rev Mol Cell Biol* 9: 464-477.
15. Kalab P, Heald R (2008) The RanGTP gradient - a GPS for the mitotic spindle. *J Cell Sci* 121: 1577-1586.
16. Wilde A, Zheng Y (1999) Stimulation of microtubule aster formation and spindle assembly by the small GTPase Ran. *Science* 284: 1359-1362.
17. Carazo-Salas RE, Gruss OJ, Mattaj IW, Karsenti E (2001) Ran-GTP coordinates regulation of microtubule nucleation and dynamics during mitotic-spindle assembly. *Nat Cell Biol* 3: 228-234.
18. Wilde A, Lizarraga SB, Zhang L, Wiese C, Gliksman NR, et al. (2001) Ran stimulates spindle assembly by altering microtubule dynamics and the balance of motor activities. *Nat Cell Biol* 3: 221-227.

19. Caudron M, Bunt G, Bastiaens P, Karsenti E (2005) Spatial coordination of spindle assembly by chromosome-mediated signaling gradients. *Science* 309: 1373-1376.
20. Li HY, Zheng Y (2004) Phosphorylation of RCC1 in mitosis is essential for producing a high RanGTP concentration on chromosomes and for spindle assembly in mammalian cells. *Genes Dev* 18: 512-527.
21. Zhang C, Goldberg MW, Moore WJ, Allen TD, Clarke PR (2002) Concentration of Ran on chromatin induces decondensation, nuclear envelope formation and nuclear pore complex assembly. *Eur J Cell Biol* 81: 623-633.
22. Arnaoutov A, Azuma Y, Ribbeck K, Joseph J, Boyarchuk Y, et al. (2005) Crm1 is a mitotic effector of Ran-GTP in somatic cells. *Nat Cell Biol* 7: 626-632.
23. Funabiki H, Murray AW (2000) The *Xenopus* chromokinesin Xkid is essential for metaphase chromosome alignment and must be degraded to allow anaphase chromosome movement. *Cell* 102: 411-424.
24. Tsai MY, Wang S, Heidinger JM, Shumaker DK, Adam SA, et al. (2006) A mitotic lamin B matrix induced by RanGTP required for spindle assembly. *Science* 311: 1887-1893.
25. Antonio C, Ferby I, Wilhelm H, Jones M, Karsenti E, et al. (2000) Xkid, a chromokinesin required for chromosome alignment on the metaphase plate. *Cell* 102: 425-435.
26. Moore W, Zhang C, Clarke PR (2002) Targeting of RCC1 to chromosomes is required for proper mitotic spindle assembly in human cells. *Curr Biol* 12: 1442-1447.
27. Arnaoutov A, Dasso M (2003) The Ran GTPase regulates kinetochore function. *Developmental cell* 5: 99-111.
28. Hutchins JR, Moore WJ, Hood FE, Wilson JS, Andrews PD, et al. (2004) Phosphorylation regulates the dynamic interaction of RCC1 with chromosomes during mitosis. *Current biology : CB* 14: 1099-1104.
29. Fornerod M, Ohno M, Yoshida M, Mattaj IW (1997) CRM1 is an export receptor for leucine-rich nuclear export signals. *Cell* 90: 1051-1060.
30. Knauer SK, Bier C, Habtemichael N, Stauber RH (2006) The Survivin-Crm1 interaction is essential for chromosomal passenger complex localization and function. *EMBO reports* 7: 1259-1265.
31. Hutten S, Kehlenbach RH (2007) CRM1-mediated nuclear export: to the pore and beyond. *Trends in cell biology* 17: 193-201.
32. Arnaoutov A, Azuma Y, Ribbeck K, Joseph J, Boyarchuk Y, et al. (2005) Crm1 is a mitotic effector of Ran-GTP in somatic cells. *Nature cell biology* 7: 626-632.
33. Torosantucci L, De Luca M, Guarguaglini G, Lavia P, Degrossi F (2008) Localized RanGTP accumulation promotes microtubule nucleation at kinetochores in somatic mammalian cells. *Molecular biology of the cell* 19: 1873-1882.
34. Zhang C, Clarke PR (2000) Chromatin-independent nuclear envelope assembly induced by Ran GTPase in *Xenopus* egg extracts. *Science* 288: 1429-1432.
35. Hetzer M, Bilbao-Cortes D, Walther TC, Gruss OJ, Mattaj IW (2000) GTP hydrolysis by Ran is required for nuclear envelope assembly. *Molecular cell* 5: 1013-1024.
36. Yuen HF, Chan KK, Grills C, Murray JT, Platt-Higgins AM, et al. (2011) Ran is a potential therapeutic target for cancer cells with molecular changes associated with activation of the PI3K/Akt/mTORC1 and Ras/MEK/ERK pathways.

Clinical cancer research : an official journal of the American Association for Cancer Research.

37. Kurisetty VV, Johnston PG, Johnston N, Erwin P, Crowe P, et al. (2008) RAN GTPase is an effector of the invasive/metastatic phenotype induced by osteopontin. *Oncogene* 27: 7139-7149.
38. Cheeseman IM, Chappie JS, Wilson-Kubalek EM, Desai A (2006) The conserved KMN network constitutes the core microtubule-binding site of the kinetochore. *Cell* 127: 983-997.
39. Sundin LJ, Guimaraes GJ, Deluca JG (2011) The NDC80 complex proteins Nuf2 and Hec1 make distinct contributions to kinetochore-microtubule attachment in mitosis. *Molecular biology of the cell* 22: 759-768.
40. Desai A, Rybina S, Muller-Reichert T, Shevchenko A, Hyman A, et al. (2003) KNL-1 directs assembly of the microtubule-binding interface of the kinetochore in *C. elegans*. *Genes & development* 17: 2421-2435.
41. McClelland ML, Kallio MJ, Barrett-Wilt GA, Kestner CA, Shabanowitz J, et al. (2004) The vertebrate Ndc80 complex contains Spc24 and Spc25 homologs, which are required to establish and maintain kinetochore-microtubule attachment. *Current biology : CB* 14: 131-137.
42. Wilson-Kubalek EM, Cheeseman IM, Yoshioka C, Desai A, Milligan RA (2008) Orientation and structure of the Ndc80 complex on the microtubule lattice. *The Journal of cell biology* 182: 1055-1061.
43. Alushin GM, Ramey VH, Pasqualato S, Ball DA, Grigorieff N, et al. (2010) The Ndc80 kinetochore complex forms oligomeric arrays along microtubules. *Nature* 467: 805-810.
44. Salmon ED, Cimini D, Cameron LA, DeLuca JG (2005) Merotelic kinetochores in mammalian tissue cells. *Philosophical transactions of the Royal Society of London Series B, Biological sciences* 360: 553-568.
45. Maiato H, DeLuca J, Salmon ED, Earnshaw WC (2004) The dynamic kinetochore-microtubule interface. *Journal of cell science* 117: 5461-5477.
46. Andrews PD, Ovechkina Y, Morrice N, Wagenbach M, Duncan K, et al. (2004) Aurora B regulates MCAK at the mitotic centromere. *Developmental cell* 6: 253-268.
47. Lan W, Zhang X, Kline-Smith SL, Rosasco SE, Barrett-Wilt GA, et al. (2004) Aurora B phosphorylates centromeric MCAK and regulates its localization and microtubule depolymerization activity. *Current biology : CB* 14: 273-286.
48. Knowlton AL, Lan W, Stukenberg PT (2006) Aurora B is enriched at merotelic attachment sites, where it regulates MCAK. *Current biology : CB* 16: 1705-1710.
49. Kelly AE, Funabiki H (2009) Correcting aberrant kinetochore microtubule attachments: an Aurora B-centric view. *Current opinion in cell biology* 21: 51-58.
50. Ditchfield C, Johnson VL, Tighe A, Ellston R, Haworth C, et al. (2003) Aurora B couples chromosome alignment with anaphase by targeting BubR1, Mad2, and Cenp-E to kinetochores. *The Journal of cell biology* 161: 267-280.
51. Lampson MA, Renduchitala K, Khodjakov A, Kapoor TM (2004) Correcting improper chromosome-spindle attachments during cell division. *Nature cell biology* 6: 232-237.
52. Oh HJ, Kim MJ, Song SJ, Kim T, Lee D, et al. (2010) MST1 limits the kinase activity of aurora B to promote stable kinetochore-microtubule attachment. *Current biology : CB* 20: 416-422.

53. Liu D, Vleugel M, Backer CB, Hori T, Fukagawa T, et al. (2010) Regulated targeting of protein phosphatase 1 to the outer kinetochore by KNL1 opposes Aurora B kinase. *The Journal of cell biology* 188: 809-820.
54. Chan YW, Jeyaprakash AA, Nigg EA, Santamaria A (2012) Aurora B controls kinetochore-microtubule attachments by inhibiting Ska complex-KMN network interaction. *The Journal of cell biology* 196: 563-571.
55. Morrow CJ, Tighe A, Johnson VL, Scott MI, Ditchfield C, et al. (2005) Bub1 and aurora B cooperate to maintain BubR1-mediated inhibition of APC/CCdc20. *Journal of cell science* 118: 3639-3652.
56. Wong CH, Chan H, Ho CY, Lai SK, Chan KS, et al. (2009) Apoptotic histone modification inhibits nuclear transport by regulating RCC1. *Nature cell biology* 11: 36-45.
57. Praskova M, Xia F, Avruch J (2008) MOBKL1A/MOBKL1B phosphorylation by MST1 and MST2 inhibits cell proliferation. *Current biology : CB* 18: 311-321.
58. Zhao B, Lei Q, Guan KL (2009) Mst out and HCC in. *Cancer cell* 16: 363-364.
59. Cheung WL, Ajiro K, Samejima K, Kloc M, Cheung P, et al. (2003) Apoptotic phosphorylation of histone H2B is mediated by mammalian sterile twenty kinase. *Cell* 113: 507-517.
60. Tedeschi A, Ciciarello M, Mangiacasale R, Roscioli E, Rensen WM, et al. (2007) RANBP1 localizes a subset of mitotic regulatory factors on spindle microtubules and regulates chromosome segregation in human cells. *J Cell Sci* 120: 3748-3761.
61. Kalab P, Pralle A, Isacoff EY, Heald R, Weis K (2006) Analysis of a RanGTP-regulated gradient in mitotic somatic cells. *Nature* 440: 697-701.
62. Uchida S, Sekiguchi T, Nishitani H, Miyauchi K, Ohtsubo M, et al. (1990) Premature chromosome condensation is induced by a point mutation in the hamster RCC1 gene. *Mol Cell Biol* 10: 577-584.
63. Nishitani H, Ohtsubo M, Yamashita K, Iida H, Pines J, et al. (1991) Loss of RCC1, a nuclear DNA-binding protein, uncouples the completion of DNA replication from the activation of cdc2 protein kinase and mitosis. *EMBO J* 10: 1555-1564.
64. Seino H, Nishitani H, Seki T, Hisamoto N, Tazunoki T, et al. (1991) RCC1 is a nuclear protein required for coupling activation of cdc2 kinase with DNA synthesis and for start of the cell cycle. *Cold Spring Harb Symp Quant Biol* 56: 367-375.
65. Dasso M (2006) Ran at kinetochores. *Biochem Soc Trans* 34: 711-715.
66. Janssen A, Medema RH (2011) Mitosis as an anti-cancer target. *Oncogene* 30: 2799-2809.
67. Malkusch W (2004) Quantitative Measurements Of FRET Using Standard Fluorescence Microscopy. *Bioscience Technology*. pp. 32-34.
68. Kalab P, Pralle A (2008) Chapter 21: Quantitative fluorescence lifetime imaging in cells as a tool to design computational models of ran-regulated reaction networks. *Methods in cell biology* 89: 541-568.
69. Li HY, Ng WP, Wong CH, Iglesias PA, Zheng Y (2007) Coordination of chromosome alignment and mitotic progression by the chromosome-based Ran signal. *Cell cycle* 6: 1886-1895.
70. Kalab P, Weis K, Heald R (2002) Visualization of a Ran-GTP gradient in interphase and mitotic *Xenopus* egg extracts. *Science* 295: 2452-2456.

71. Uchida S, Sekiguchi T, Nishitani H, Miyauchi K, Ohtsubo M, et al. (1990) Premature chromosome condensation is induced by a point mutation in the hamster RCC1 gene. *Molecular and cellular biology* 10: 577-584.
72. Brinkley BR, Cartwright J, Jr. (1975) Cold-labile and cold-stable microtubules in the mitotic spindle of mammalian cells. *Annals of the New York Academy of Sciences* 253: 428-439.
73. Musacchio A, Hardwick KG (2002) The spindle checkpoint: structural insights into dynamic signalling. *Nature reviews Molecular cell biology* 3: 731-741.
74. Kulukian A, Han JS, Cleveland DW (2009) Unattached kinetochores catalyze production of an anaphase inhibitor that requires a Mad2 template to prime Cdc20 for BubR1 binding. *Developmental cell* 16: 105-117.
75. Yasui Y, Urano T, Kawajiri A, Nagata K, Tatsuka M, et al. (2004) Autophosphorylation of a newly identified site of Aurora-B is indispensable for cytokinesis. *The Journal of biological chemistry* 279: 12997-13003.
76. Girdler F, Sessa F, Patercoli S, Villa F, Musacchio A, et al. (2008) Molecular basis of drug resistance in aurora kinases. *Chemistry & biology* 15: 552-562.
77. Santaguida S, Tighe A, D'Alise AM, Taylor SS, Musacchio A (2010) Dissecting the role of MPS1 in chromosome biorientation and the spindle checkpoint through the small molecule inhibitor reversine. *The Journal of cell biology* 190: 73-87.
78. Akiyoshi B, Sarangapani KK, Powers AF, Nelson CR, Reichow SL, et al. (2010) Tension directly stabilizes reconstituted kinetochore-microtubule attachments. *Nature* 468: 576-579.
79. Cimini D, Wan X, Hirel CB, Salmon ED (2006) Aurora kinase promotes turnover of kinetochore microtubules to reduce chromosome segregation errors. *Current biology : CB* 16: 1711-1718.
80. Santaguida S, Vernieri C, Villa F, Ciliberto A, Musacchio A (2011) Evidence that Aurora B is implicated in spindle checkpoint signalling independently of error correction. *The EMBO journal* 30: 1508-1519.
81. Maia AF, Feijao T, Vromans MJ, Sunkel CE, Lens SM (2010) Aurora B kinase cooperates with CENP-E to promote timely anaphase onset. *Chromosoma* 119: 405-413.
82. Clarke PR, Zhang C (2008) Spatial and temporal coordination of mitosis by Ran GTPase. *Nature reviews Molecular cell biology* 9: 464-477.
83. Fuller BG (2010) Self-organization of intracellular gradients during mitosis. *Cell division* 5: 5.
84. Chan KS, Wong CH, Huang YF, Li HY (2010) Survivin withdrawal by nuclear export failure as a physiological switch to commit cells to apoptosis. *Cell death & disease* 1: e57.
85. Carazo-Salas RE, Gruss OJ, Mattaj IW, Karsenti E (2001) Ran-GTP coordinates regulation of microtubule nucleation and dynamics during mitotic-spindle assembly. *Nature cell biology* 3: 228-234.
86. Wilde A, Lizarraga SB, Zhang L, Wiese C, Gliksman NR, et al. (2001) Ran stimulates spindle assembly by altering microtubule dynamics and the balance of motor activities. *Nature cell biology* 3: 221-227.
87. Tatsuka M, Katayama H, Ota T, Tanaka T, Odashima S, et al. (1998) Multinuclearity and increased ploidy caused by overexpression of the aurora- and Ipl1-like midbody-associated protein mitotic kinase in human cancer cells. *Cancer research* 58: 4811-4816.

88. Lenart P, Petronczki M, Steegmaier M, Di Fiore B, Lipp JJ, et al. (2007) The small-molecule inhibitor BI 2536 reveals novel insights into mitotic roles of polo-like kinase 1. *Current biology : CB* 17: 304-315.
89. Marcus AI, Peters U, Thomas SL, Garrett S, Zelnak A, et al. (2005) Mitotic kinesin inhibitors induce mitotic arrest and cell death in Taxol-resistant and -sensitive cancer cells. *The Journal of biological chemistry* 280: 11569-11577.
90. Harrington EA, Bebbington D, Moore J, Rasmussen RK, Ajose-Adeogun AO, et al. (2004) VX-680, a potent and selective small-molecule inhibitor of the Aurora kinases, suppresses tumor growth in vivo. *Nature medicine* 10: 262-267.
91. Bekier ME, Fischbach R, Lee J, Taylor WR (2009) Length of mitotic arrest induced by microtubule-stabilizing drugs determines cell death after mitotic exit. *Molecular cancer therapeutics* 8: 1646-1654.
92. Xia F, Canovas PM, Guadagno TM, Altieri DC (2008) A survivin-ran complex regulates spindle formation in tumor cells. *Molecular and cellular biology* 28: 5299-5311.
93. Navarro MS, Bachant J (2008) RanBP2: a tumor suppressor with a new twist on TopoII, SUMO, and centromeres. *Cancer cell* 13: 293-295.
94. Doherty KJ, McKay C, Chan KK, El-Tanani MK (2011) RAN GTPase as a Target for Cancer Therapy: Ran Binding Proteins. *Current molecular medicine* 11: 686-695.